Master's thesis

NTNU
Norwegian University of Science and Technology
Faculty of Natural Sciences
Department of Biology

Elisabeth Alice Snijder

Investigating abiotic and biotic factors related to the growth of bryozoans on kelp lamina

Master's thesis in Ocean Resources
Supervisor: Glaucia Moreira Fragoso
Co-supervisor: David Aldridge, Ole Jacob Broch, Geir Johnsen
May 2024

NTNU
Norwegian University of
Science and Technology

Elisabeth Alice Snijder

Investigating abiotic and biotic factors related to the growth of bryozoans on kelp lamina

Master's thesis in Ocean Resources
Supervisor: Glaucia Moreira Fragoso
Co-supervisor: David Aldridge, Ole Jacob Broch, Geir Johnsen
May 2024

Norwegian University of Science and Technology
Faculty of Natural Sciences
Department of Biology

NTNU
Norwegian University of
Science and Technology

Abstract

Biofouling of bryozoan colonies affects the quality of cultivated seaweed and thereby shortens the growth season, reducing the profits for the seaweed industry. In Norway, there are two main bryozoan species that impact the quality of cultivated kelp, *Membranipora membranacea* and *Electra pilosa* that settle and encrust on the surface of the kelp species *Saccharina latissima* (Phaeophyceae, brown algae). This study investigated the environmental variables, in particular seawater temperature, turbidity (particle concentrations), weather conditions and the timing and concentration of phytoplankton blooms (chlorophyll *a*), that influence the settlement and growth of encrusting bryozoan colonies on the kelp lamina. This study also explored the use of a simple, low-cost flatbed scanner to detect early settlement stages and to quantify bryozoan coverage on the kelp lamina. Environmental data were collected from a seaweed farm in Frøya, Norway, from February 2023 until the end of June 2023. Time-series data (every 10 minutes) of temperature, in situ chlorophyll *a*, and turbidity were collected for the whole cultivation period. Also, vertical depth profile measurements were conducted and water samples were collected for the analysis of ammonium and nitrate and in vitro [Chl *a*] (in total 9 sample dates). Furthermore, kelp lamina samples were collected for quantification of bryozoan colony coverage from the 25^{th} of April until the 29^{th} of June (in total 7 sample dates) from two cultivation lines (deployment time was October 2022 and the other January 2023).

The results showed that bryozoan larvae start settling at the end of April, approximately 3 weeks after the peak of the spring bloom (chlorophyll *a* biomass > 2 mg m^{-3} from the time-series sensor). The abundance of colonies gradually increased from May until the end of June and the percentage of bryozoan coverage exponentially increased in June. The observed colony size also increased exponentially in time, and the smallest colony size had the highest abundance in time. A higher percentage coverage was observed for the line that was deployed in October 2022 compared with the line that was deployed in January 2023. Settlement of bryozoan larvae and pre-ancestrula stages showed peaks in abundance when there was a sharp increase in temperature and was low during a period with high wind speed and low daily average irradiance, indicating that storms negatively affect the settlement. Percentage coverage showed a strong correlation ($p < 0.05$) with the average temperature. Moreover, the cumulative temperature was shown to have an effect ($p < 0.05$) on the percentage coverage and the colony abundance with respect to every previous sampling date. The coverage was not linearly related with chlorophyll *a*, suggesting that, as long as there is enough food (in the case of this study chlorophyll $a \geq 2$ mg m^{-3}), other factors (e.g. temperature, currents) interplay.

Sammendrag

Begroing av mosdyrkolonier påvirker kvaliteten på dyrket tare og forkorter vekstsesongen og reduserer inntjeningen for makroalgeindustrien. I Norge er det to hovedtyper mosdyr som påvirker kvaliteten på dyrket tare, *Membranipora membranacea* og *Electra pilosa*, som setter seg på overflaten av tarearten *Saccharina latissima* (Phaeophyceae, brunalger). Denne studien undersøkte miljøparameterne som påvirker påslag og vekst i av mosdyrkolonier på tarebladene. Det er lagt særlig vekt på temperatur, turbiditet (partikkelkonsentrasjon), værforhold samt tidspunkt og konsentrasjon av planteplanktonblomstring (klorofyll *a*). Denne studien undersøkte også bruk av en enkel og rimelig skanner til å påvise påslag av mosdyrlaver og å kvantifisere mosdyrbegroingen på tarebladene. Miljødata ble samlet inn fra et taredyrkingsanlegg ved Frøya, Norge, fra februar 2023 til slutten av juni 2023. Tidsseriedata (hvert 10. minutt) for temperatur, in situ klorofyll *a* og turbiditet ble samlet for hele dyrkingsperioden. I tillegg ble vertikale dybdeprofilmålinger gjennomført og vannprøver ble samlet inn for å analysere ammonium, nitrat og in vitro klorofyll *a* (totalt ni registreringsdatoer). Videre ble tarebladprøver samlet inn for å kvantifisere arealdekningsgraden av mosdyrkolonier fra 25. april til 29. juni (totalt sju registreringsdatoer) fra to tareliner (utsettingstidspunktene var oktober 2022 og januar 2023).

Resultatene viste at mosdyrlarvene begynte å sette seg på slutten av april, omtrent tre uker etter toppen av våroppblomstringen (klorofyll *a* biomasse > 2 mg m^{-3} fra tidsseriesensoren). Antall kolonier økter gradvis fra mai til slutten av juni, og arealdekningen av mosdyrbegroing økte eksponentielt i juni. Observert kolonistørrelse økte også eksponentielt med tiden og den minste kolonistørrelsen hadde størst antall. Høyere andel begroing ble observert på tarelina som ble satt ut i oktober 2022 enn tarelina som ble satt ut i januar 2023. Flest mosdyrpåslag ble observert når det var en rask temperaturøkning, men påslaget var lavt i perioder med høy vindhastighet og lav gjennomsnittlig daglig lysinnstråling. Dette tyder på at stormer påvirker mosdyrpåslaget negativt. Prosentvis arealdekning var sterkt korrelert ($p < 0.05$) med gjennomsnittstemperaturen. Videre viste kumulativ temperatur seg å ha en effekt ($p < 0.05$) på prosentvis arealdekning og antall kolonier med hensyn til prøvetakingsdato. Arealdekningen var ikke lineært relatert til klorofyll *a*, noe som tyder på at så lenge det er nok mat (i denne studien klorofyll *a* ≥ 2 mg m^{-3}), spiller også andre faktorer (f. eks. temperatur, vannstrøm) inn.

Acknowledgments

The MSc project has been completed at the Department of Biology at the Norwegian University of Science and Technology in the period from December 2022 to May 2024. This thesis was part of the following project: "Autonomous underwater monitoring of kelp-farm biomass, growth, health and biofouling using optical sensors", MoniTARE (315514) (2021-2025) and funded by the Research Council of Norway (RCN). Access to the kelp farm in Frøya was provided by Seaweed Solutions. Labwork was conducted at Trondheim Biologiske Stasjon.

I would like to express my sincere gratitude to my supervisor, Glaucia Fragoso, for giving me the possibility to join the moniTARE project and conduct my thesis project in seaweed aquaculture. I learned so much from you and enjoyed working together with you. Thank you for all the support and academic insights. In addition, I would like to thank my co-supervisors, David Aldridge, Ole Jacob Broch and Geir Johnsen for all the support, feedback and interesting discussions during this project. A special thanks to Artur Zolich, for helping me around at the very first start of exploring the method for this project.

Thank you, all SES people, for the help during the fieldwork, the interesting talks, and the part-time job I got during my time here in Trondheim. I always enjoyed being there, and it was really inspiring to see the dedication of the whole team. A big thanks to the KELPie team, Nalia and Adrian. I really enjoyed fieldwork and lab work together, even the hectic parts. Håvard thank you for helping me translate the abstract and also for being the best roommate.

My gratitude also goes to everyone at TBS. It was a gift to work in such a nice environment. Hedda, you are the best and thank you for all the fun moments and blubs together. I am going to miss you so much.

Finally, Jelte, een mega dankjewel to you for the endless discussions and for helping me make the script for the method. Without your help, I would not have been able to get this result. Thank you so much, family, mam, pap, Sien, Noor, and friends in the Netherlands, for the support and love during my time here in Trondheim.

May 2024, Trondheim

Els Snijder

Contents

List of Figures

List of Tables

Abbreviations

List of all abbreviations in alphabetic order:

- **CCD** Charged Coupled Device (type of scanner)
- **Chl *a*** Chlorophyll *a*
- **[Chl *a*]** Chlorophyll *a* concentration in μg L^{-1} or mg m^{-3}
- **CIS** Contact Imaging Sensor (type of scanner)
- **CTD** Conductivity, Temperature (°C) and Depth. Conductivity is used as a measure to estimate the Salinity levels (ppm) in the water column. The depth is measured in pressure (decibar) where 1 decibar is 1 meter in depth.
- **DPI** Dots per inch in an image
- **FChl *a*** chlorophyll *a* fluorescence
- **FTU** Formazin Turbidity Unit. This is the unit of turbidity measured with the sensor.
- **NTNU** Norwegian University of Science and Technology
- **SVG** Scalable Vector Graphics (Vector-based image file format)
- **TBS** Trondheim Biologiske Stasjon
- **TIFF** Tag Image File Format (a file format to store high-quality images)

Chapter 1

Introduction

1.1 Seaweed farming

As the world's population continues to grow rapidly, and so does its demand for food, there is an urgent need for more sustainable and alternative protein-source food products (FAO, 2021). Seaweed, also known as macroalgae, is becoming an increasingly viable option in this regard. It can be used for many applications including animal feed, fertilizers, cosmetics, human food and the production of proteins (Koesling et al., 2021; Skjermo et al., 2014). Seaweed is seen as a potential sustainable food source for human consumption, as carbon emissions are low during the production cycle because the macroalgae convert CO_2 into organic carbon through photosynthesis (Thomas et al., 2021). Besides, seaweed is healthy since it has a high nutritional value, contains many essential minerals and vitamins, and it does not need any fertilizers or chemicals to grow (Lomartire et al., 2021). Seaweed can be harvested in the wild but can also be produced through aquaculture, which is also called seaweed farming or cultivation. Seaweed farming has different stages in the production cycle and can be farmed on land, but for some cultivation methods, the grow-out phase is in the sea, where the seaweed is growing on suspended long lines (Matsson, 2020; Verdegem et al., 2023, figure 1.1.1).

In Asian countries, seaweed is a common product in their traditional diet and this has made seaweed farming a developed sector there. They are responsible for 99% of the global seaweed production (FAO, 2022). The interest in seaweed farming is increasing in Norway as well. The current commercial production in Norway has increased from 0 tons of seaweed in 2014 to 221 metric tons in 2022, with a total of 522 permits in 2023 (Directorate of Fisheries, 2023). It is mentioned by the Norwegian Seaweed Association that the yearly production is even higher (around 400 tonnes per year), and this difference is because many companies are still in an early development stage and are not active yet in a commercial way (Albrecht, 2023). According to the Norwegian Seaweed Association, the expected production in 2023 was 500 tons (Norwegian Seaweed Association, pers comm), and it is expected that commercial production will keep increasing with time. The perspectives regarding industrial developments and farming seaweed under different conditions, such as at offshore locations and/or in synergies with fish farms in the future, are overall positive (Stévant et al., 2017).

Norway has a long coastline and optimal climate conditions for seaweed aquaculture (Forbord et al., 2020; Skjermo et al., 2014). *Saccharina latissima* (Linnaeus) is a brown

seaweed (kelp) species native to the Norwegian coast and is suitable for seaweed farming as it has a rapid growth rate and a healthy nutritional composition with low-fat, high carbohydrate, and varying protein content (Bak et al., 2018; Rioux et al., 2017; Saifullah et al., 2021; Sjøtun, 1993). As the cultivation method of this species is already well known, farmers are particularly interested in using this species in aquaculture (Forbord et al., 2018; Saether et al., 2024).

Figure 1.1.1: *S. latissima* growing at long lines in the sea at the farm of Seaweed Solutions AS in Frøya, mid-Norway (Image from Seaweed Solutions).

1.2 Biofouling

Despite its potential, the seaweed production sector is not yet profitable. Parts of the production cycle, especially harvesting and monitoring, are still labour-intensive and time-consuming because of a lack of automation. Therefore, farmers are trying to minimise production costs by having the maximum biomass yield of seaweed harvested where the seaweed still has a good quality. One main challenge in the sector that limits the maximum biomass harvest of seaweed in Norway, is the attachment of small organisms to the seaweed, also called biofouling. Biofouling can lead to some negative impacts on the quality of seaweed. Fouling species can block the uptake of light and nutrients for the seaweed and can also cause physical damage to the lamina, resulting in a decrease in quality and loss of commercial value (Bannister et al., 2019). One biofouling species that mainly settles and encrusts *S. latissima* are the marine invertebrate bryozoans. Bryozoans, sometimes called 'moss animals', form large colonies on the kelp lamina and make

the lamina fragile and more susceptible to break (Førde et al., 2016; Santagata, 2015). Too much fouling makes the seaweed unsuitable to use for human consumption.

1.3 The life cycle of bryozoans

There is a significant lack of studies on the life cycle histories of bryozoans (Shevchenko et al., 2020). The lifecycle of bryozoans is complex as it has different life stages, including a planktonic larval stage in the water, and a benthic sessile stage, where they encrust the substrate and form colonies. A general overview of the bryozoans (phylum Ectoprocta, clade II Polyzoa in clade Lophotrochozoan) is given by Hickman et al. (2017). Bryozoans are aquatic invertebrate animals that principally encrust surfaces such as rocks and seaweed. Most of the bryozoan species are colony builders during their sessile period, where one member of the colony, called a zooid, is mainly not smaller than 0.5 mm. Every colony starts with one settled and metamorphosed primary zooid called the ancestrula. The ancestrula undergoes asexual budding to produce other zooids of the colony. These zooids live in secreted small containers forming a calcareous exoskeleton called zoecium (figure 1.3.1a). The zoecium and the body wall of the animal together form the case-forming cystid.

Each zooid consists of a feeding polypide that includes the lophophore (tentacles), digestive tract, muscles, and nerve centres (figure 1.3.1b). Bryozoan colonies are suspension feeders and feed with their lophophores by extending them into the surrounding water to collect microscopic microorganisms, including protozoans and phytoplankton. The food size depends on the size of the bryozoan mouth, but it is mainly phytoplankton smaller than 50 μm in diameter, particularly flagellates (Winston, 1977). Bryozoans do not contain respiratory, vascular, or excretory organs, and the exchange of gas happens through the body surface (Hickman et al., 2017).

In Norwegian kelp farms, there are two main bryozoan species that settle and encrust *S. latissima*: *Membranipora membranacea* and *Electra pilosa*. These two species are both in the class Gymnolaemata and order Cheilostomatida. Both are hermaphroditic and have a relatively long-lived planktotrophic larval stage, but they differ in colony form and development of the ancestrula (Ryland and Stebbing, 1971).

1.3.1 From egg development to cyphonaute

Sexual reproduction of bryozoans starts with fertilization by spermatozoa from another zooid. Fertilization happens in the intertentacular organ and the fertilized yolk-poor eggs are discharged into the sea (figure 1.3.1b). For both *M. membranacea* and *E. pilosa*, the number of eggs produced in one reproductive period is large (Franzén, 1977). The eggs are hatched and are developed into pelagic, obligatory planktotrophic larvae, known as cyphonautes (Franzén, 1977). The larva, a filter feeder, continues to grow as long as there is food available and further develops into a fully grown cyphonaute larva. Cyphonaute larvae have a functional gut and feed by creating a feeding current with their cilia. They feed on small microscopic organisms of phytoplankton during their larval stage in the water (Ryland and Stebbing, 1971). Fully developed *M. membranacea* larvae are bigger (length of 750 - 850 µm) compared to the larvae of *E. pilosa* (length of 400 - 500 µm) and tend to be more transparent (Ryland and Stebbing, 1971).

For *M. membranacea*, the production of gametes starts in spring, and fertilized eggs are discharged continuously until mid-summer (Burridge, 2012). It is mentioned that for *E. pilosa*, gametes are produced mainly in late summer and cyphonautes are present as plankton throughout the year (Ryland, 1965; Shevchenko et al., 2020).

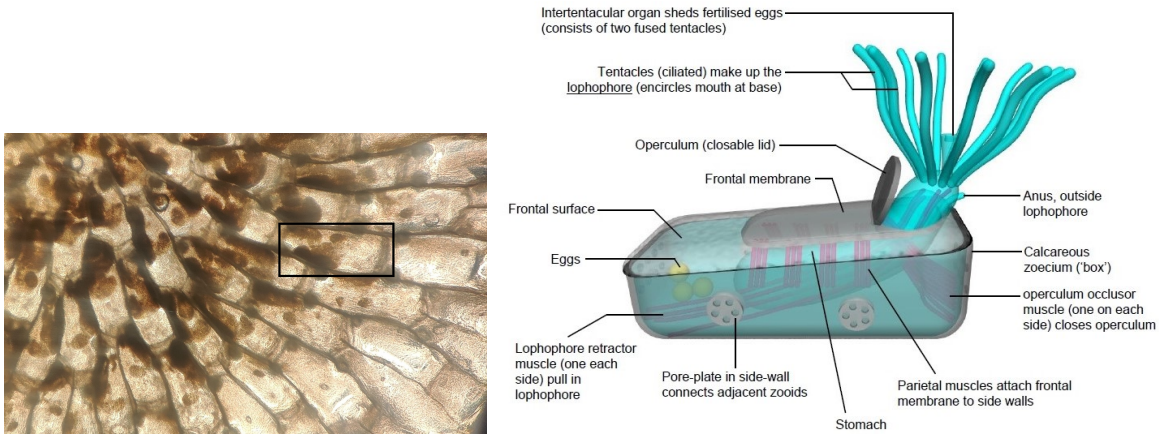

(a) **(b)**

Figure 1.3.1: *Membranipora membranacea* through the microscope with the black box indicating one zoecium (a) and the anatomy of the bryozoan based on the cheilostome order (b). Image from b is retrieved from www.cronodon.com

1.3.2 From larva settlement to metamorphosis

Populations of *M. membranacea* and *E. pilosa* larvae rely on phytoplankton for food and, therefore, are able to remain in the water for days or weeks before settling on the kelp (Soule and Soule, 1977). It is known that *M. membranacea* larvae can stay in the water for up to four weeks before settling on the kelp (Yoshioka, 1982). Cyphonaute larvae are able to survive in their planktonic larval stage for a long period until they become competent and find a substrate that is suitable enough to settle (Hadfield et al., 2001). *E. pilosa* tend to settle two months after hatching from the egg (Ryland and Stebbing, 1971). When a cyphonaute larva settles, it is actively testing the surface. It holds fast to the substrate by secretion from the pyriform gland. Right before settlement takes place, the cyphonaute larva, with its sail-like shape, orients itself on the substrate against the direction of water flow until it suddenly quickly moves in circles and turns its adhesive sac. The positive rheotropism of the larvae (growth and settlement in the direction of water flow) suggests that the alignment is likely to be adopted to ensure the best assimilation of food by the colony (Ryland and Stebbing, 1971). The valves, then, separate and are pulled down on the substrate and the larva is ready to start its metamorphosis into an ancestrula, the first zooid of the bryozoan colony, and the transparent valves fall away sometime later (Atkins, 1955).

Metamorphosis is the period of all events that happen from the settlement of the competent larva until it reaches its ancestrula stage (Zimmer and Woollacott, 1977). Metamorphosis for both species has two stages: the first stage, the pre-ancestrula stage, takes a few minutes, and the second stage, which lasts 1 to 6 days, is the stage where the pre-ancestrula transforms into an ancestrula that contains a fully developed zooid.

The duration of the second phase of the metamorphosis depends on the species and temperature (Zimmer and Woollacott, 1977). One difference between the two species is that *M. membranacea* produces a twin ancestrula in the second stage of metamorphosis with two primary zooids (Atkins, 1955; Stricker, 1989). The term pre-ancestrulae is used in this project, to refer to new bryozoan larvae that settled but have not metamorphosed into a fully developed (twin) ancestrula yet. Settlement and pre-ancestrulae are described when the larvae clearly show a triangular shape (settlement) or when the valve has already fallen away but metamorphosis is still happening because it does not show a clear septum yet (pre-ancestrula, figure 2.2.4, Stricker, 1989). It is known that the cyphonaute larvae tend to settle on the newest part of the lamina, called the meristem (Denley et al., 2014; Matsson, 2020).

1.3.3 Asexual reproduction (colony growth)

Once the zooid is fully developed, it reproduces asexually forming an encrusting colony. *Membranipora membranacea* is sexually reproductive 40 days after settlement when undisturbed (Harvell and Helling, 1993), and this species has a preference for kelp lamina (Hayward and Ryland, 2017). *Electra pilosa* tend to have slower colony growth rates compared with *M. membranacea* and also has an overall smaller colony size on the kelp lamina (Yorke and Metaxas, 2011). *Electra pilosa* makes star-shaped colonies, whereas *M. membranacea* has circled-shaped colonies (figure 1.3.2). Some colonies overwinter and provide gametes for the next spring (M. Saunders and Metaxas, 2009; Shevchenko et al., 2020), so the life cycle can repeat itself again (figure 1.3.2). The colony life span for *E. pilosa* in the White Sea is estimated to be 13 months (Shevchenko et al., 2020).

An overview of the life cycle of *M. membranacea* and *E. pilosa* in the spring and summer

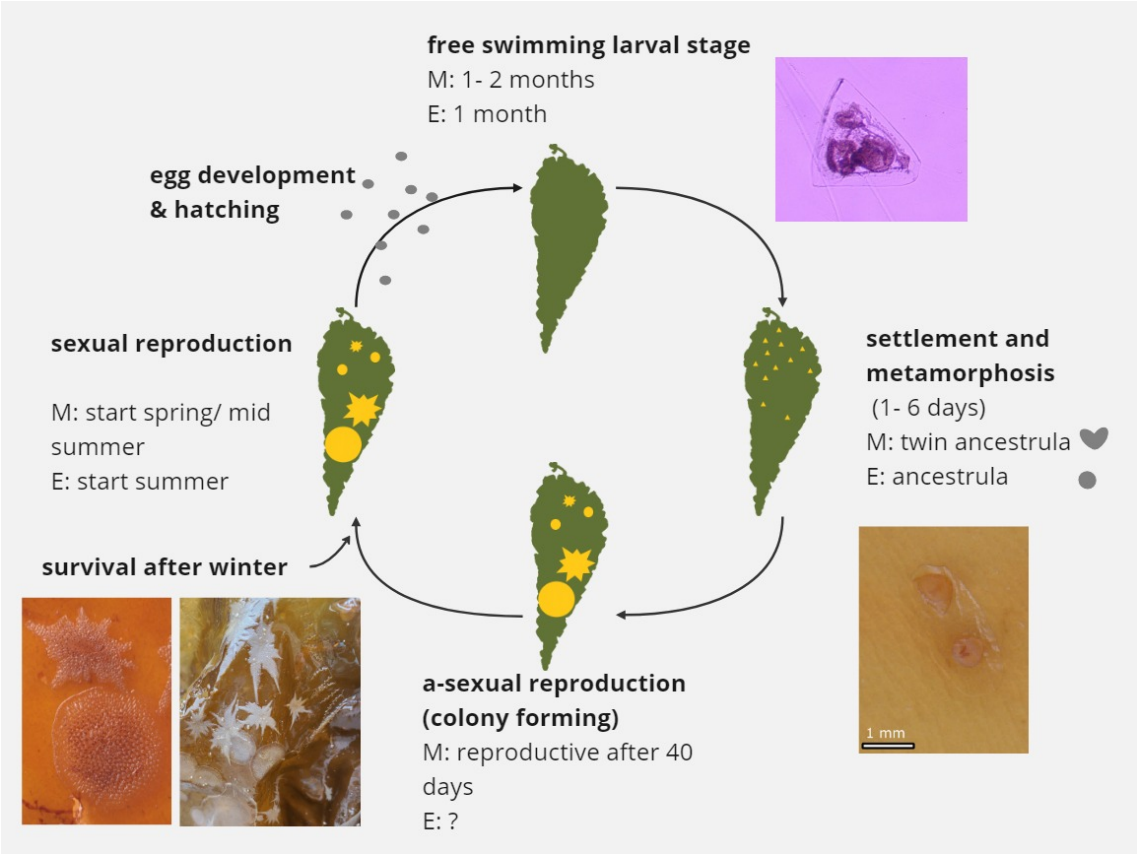

Figure 1.3.2: The life cycle of bryozoans *M. membranacea* (M) and *E. pilosa* (E) based on references in section 1.3. Sexual reproduction starts approximately between spring (end of March) and mid-summer for *M. membranacea* and approximately in summer for *E pilosa*. Egg development (indicating the grey dots), hatching, settlement and colony forming take place continuously until the end of autumn approximately. Some colonies survive the winter and provide gametes for the next spring.

1.4 Settlement and growth in combination with the environment

Førde et al. (2016) found that the larvae of the *M. membranacea* in mid-Norway (Frøya) start settling on the kelp in mid-June, followed by rapid growth of the colonies in late June and July. The seawater temperature increase for this period was approximately from 8 °C to 12 °C (Førde, 2014). However, nowadays local seaweed farmers from Trøndelag (mid-Norway) usually observe settlement already between mid-May and the beginning of June. The growth of colonies is known to increase with increasing seasonal temperature (M. Saunders and Metaxas, 2009). M. Saunders and Metaxas (2009) observed that the growth rates of the colonies of *M. membranacea* had a positive relationship with temperature, and colony size increased exponentially over temperature ranges between 5.7 °C and 16.2 °C. The study also observed an interaction effect with temperature and food, and at higher temperatures (11 °C - 14 °C), the growth rate was lower when food availability was limited.

The timing of settlement of the larvae on the substrate can be affected by different environmental parameters. Shevchenko et al. (2020) observed that *E. pilosa* in the White Sea started settling one month later (around the end of June) compared to another bryozoan (*Callopora craticula*) larva type. The study expected that this was because the abundance of phytoplankton was too low in early summer, which resulted in not enough food for the colonies to support the start of sexual reproduction and the feeding of the larva. Settlement of bryozoan larvae tends to be affected by depth and temperature. M. Saunders and Metaxas (2007) showed that settlement abundance was the highest in early autumn at deeper depths and also increased after a warmer winter.

Temperature induces larval settlement. However, other environmental factors and cues, such as food availability (high phytoplankton abundance), chemical signalling from bacterial biofilms and spectral changes in light have also been considered. Light has been suggested as a factor that induces larval hatching and may coincide with the time when the phytoplankton bloom is at its peak (Ström, 1977).

1.5 Quantifying bryozoan coverage

It would be beneficial for farmers to have an estimation of when the larvae of the bryozoans start to settle and how quickly the colonies develop on the lamina. This makes it possible to harvest before the seaweed becomes so overgrown by bryozoan colonies that it is not suitable for selling as a high-value product (e.g. human consumption). As of now, the environmental factors that trigger larva settlement and rapid growth rate of bryozoan colonies on the kelp in a cultivation farm are not well understood. Besides, the degree of biofouling is expressed on a qualitative scale (0- no fouling, 1- little fouling to 4-extremely fouled), and the first settlement is determined by looking at random spots on the kelp with a magnifying glass. These actual values are arbitrary and may vary from farmer to farmer which means that accurate data regarding coverage and size of colonies is not achieved. Because of this, no exact comparison can be made between different farming locations.

The lack of high-resolution data (frequent time registrations of bryozoan growth) and accurate information about bryozoan colony growth on the kelp lamina makes it difficult to predict how fast they will spread in the farm. Several methods have been developed to obtain a quantification of bryozoan coverage, such as using a grid to count the area of bryozoan coverage on the lamina (Matsson et al., 2019) or digitally by using a light table and a camera (Førde et al., 2016). Cohen (2019) induced fluorescence in kelp with Ultraviolet Radiation in a dark room to improve detection. Furthermore, Vassbotn Kamfjord (2002) used a customized photography chamber where the kelp lamina covered with bryozoans could be kept in the seawater while taking images of the colonies. Also, trials are done with the use of calcein ($C_{30}H_{26}N_2O_{13}$), a fluorescent dye, to mark the growth and ageing of bryozoans (Thomason, 2023). However, these methods are only effective for fully metamorphosed specimens and clear colonization. Moreover, the use of a camera in the methods mentioned above provided low-resolution images and was applied to kelp that already showed high degrees of colonization with a low-quality value for market purposes. The first settlement of the bryozoan larvae on the kelp lamina was not observed as the larvae are too small to detect with the human eye or camera. Detection and quantification of these early stages (settled larvae and pre-ancestrulae < 1

mm) is crucial information for farmers to have for predictive purposes of colony growth and to establish a grade level where they are still able to sell their product for other market purposes (e.g. for animal feed) when small colonies are present.

In this project, scanning of seaweed with an A4 flatbed scanner is conducted as a potential method to detect and digitize the distinct stages of bryozoan settlement and growth on the kelp lamina. The images from the scans were used to quantify the settlement of bryozoan larvae on the kelp, the total bryozoan colony coverage and the sizes (area) of colonies, settled larvae and pre-ancestrulae per specimen. The use of a scanner ensures that the setup easily remains the same for every scanned image. Besides, the distance between the scanned lamina and the light source of the scanner is short, and when it is known which scan resolution is used during scanning, it is possible to determine the size of the bryozoan colonies on the kelp.

1.6 Aims and objectives

The first aim of this study is to explore a new method to easily estimate bryozoan coverage on the kelp lamina and colony size. The second aim is to investigate environmental variables such as temperature, turbidity, chlorophyll *a* (Chl *a*), wind and light, that influence the growth of bryozoan colonies on the kelp lamina. This has been approached by:

1. Taking samples of *S. latissima* specimens from the moment the larvae settle (late April) until the end of June when bryozoans are expected to completely cover the lamina (7 sample dates in this period in total).

2. Collecting environmental data (temperature, Chl *a*, turbidity, wind speed, irradiance, and nutrients) from a seaweed farm located in Frøya for the whole cultivation period.

3. Exploring image scanning of the algal lamina with a simple flatbed scanner as a method to produce pictures that easily distinguish the bryozoan settlement and bryozoan colonies from the lamina.

4. Analysis of the environmental variables and bryozoan colony coverage and size data.

The hypothesis in this project is that temperature will be the main variable influencing bryozoan growth. A faster increase in seasonal temperature (6 °C - 12 °C) allows a higher growth rate of the bryozoan colonies considering a minimum of food availability (phytoplankton abundance) (M. Saunders and Metaxas, 2009; Shevchenko et al., 2020). It is predicted that within the season, a higher cumulative temperature (degree×day) will give a higher percentage bryozoan coverage. Furthermore, Chl *a* should be at least above 1 mg m^{-3} for the bryozoan larvae to settle and grow as Chl *a* can be considered as a proxy for food that is available for the bryozoan colonies to eat.

Chapter 2

Materials and Methods

2.1 Data collection

The fieldwork in this study took place from February to June 2023 at Måsskjæra (63°44.617' N 8°52.756'E), a seaweed farm located near the island of Frøya and owned by Seaweed Solutions (SES) AS (figure 2.1.1). Frøya is an island along the coast of mid-Norway in the Froan archipelago, where winds and tidal currents cause strong mixing of the water. This makes this area rich in terms of primary productivity and biological diversity (Fragoso et al., 2019; Sætre, 2007). The oceanographic dynamics of this area are characterised by the Norwegian Coastal Current (NCC), a surface water mass originating from freshwater runoffs from fjords, and the Norwegian Atlantic Current (NAC), which lies beneath the NCC and brings warm and nutrient-rich water to the area during mixing events (Sætre, 2007).

2.1.1 Kelp sampling and vertical depth profile measurements

To obtain environmental information of the area, vertical depth profile measurements occurred at one station inside the farm (station MI, bottom depth around 10 meters) (figure 2.1.1). This was done every two weeks from mid-February until late June. In total, nine sampling dates for the environmental data were selected over the period depending on weather conditions (table 2.1.1). For this, a CTD instrument with a Chl *a* fluorometer (model SD204 SAIV A/S^{tm}) was used to obtain a vertical depth profile (3x up and down) of temperature (°C), salinity (conductivity), turbidity (FTU) and in situ chlorophyll *a* concentrations (mg m^{-3}) in the farm.

For the quantification of bryozoan coverage on the kelp lamina, specimens of *S. latissima* from two distinct cultivation lines were collected, where one line was deployed in October 2022 and the other line in January 2023. The specimens were collected from late April until the end of June. In total, there were seven sampling dates, and the sample dates were based on weather conditions and the availability of the farmers to collect the samples. On every sample date, five specimens from each deployment line were taken (table 2.1.1). The samples were rolled up in aluminium foil, put into plastic bags, stored in dry ice (-80 °C) for transportation, and later stored in the freezer at -20 °C at Trondheim Biologiske Stasjon (TBS).

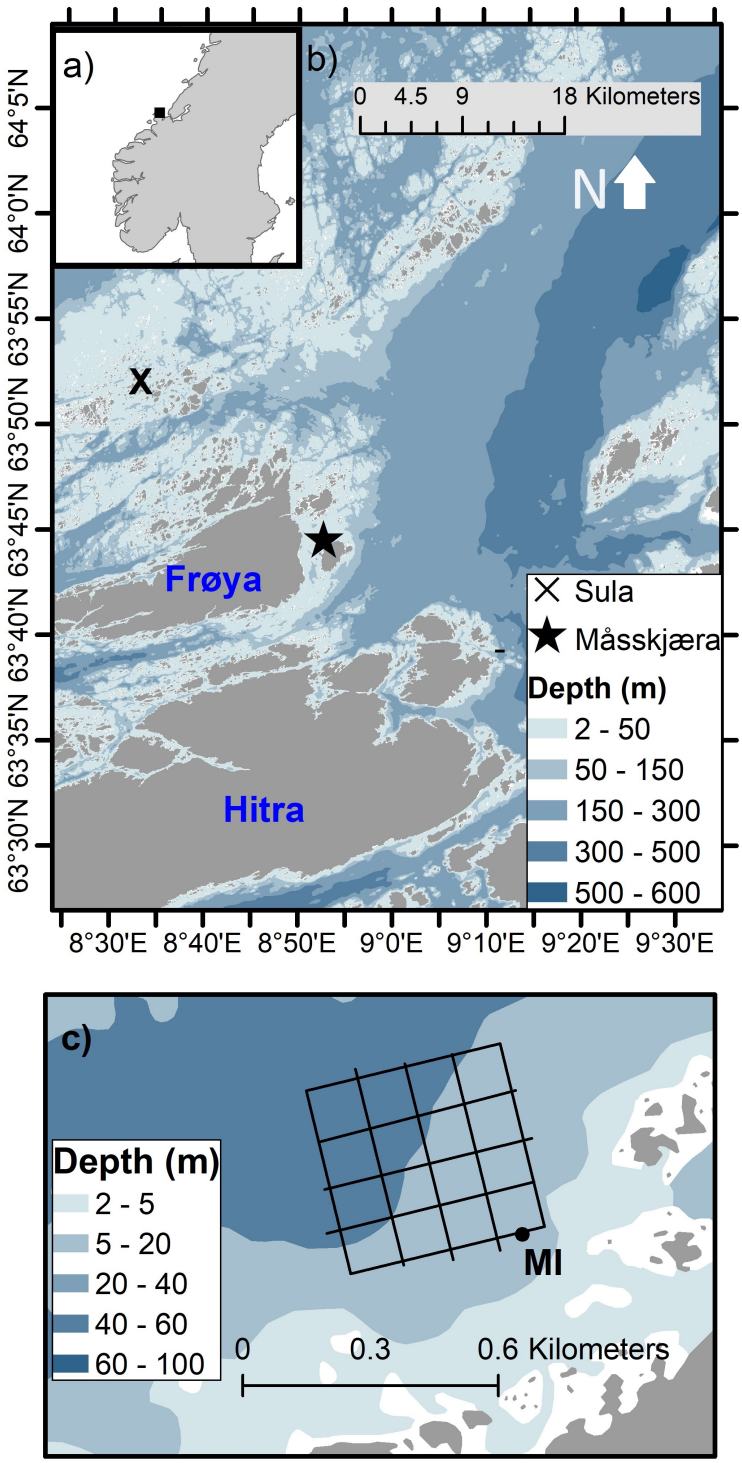

Figure 2.1.1: Location of the farm in a) the Norwegian coast (black square) and b) near Frøya island (star symbol). c) MI, Location of the station inside the farm. X indicates the Sula station where wind data is retrieved from (Norwegian Centre for Climate Services, n.d.). The figure is made in GIS (Fragoso pers comm, 2024).

Date	**CTD & Water Sampling**	**nr. replicates from the line deployed in Oct 22**	**nr. of replicates from the line deployed in Jan 23**
15-02	x	-	-
16-03	x	-	-
29-03	x	-	-
18-04	x	-	-
25-04	x	3	0
10-05	x	5	5
15-05	-	5	5
23-05	x	5	5
07-06	x	5	5
15-06	-	5	5
29-06	x	5	5

Table 2.1.1: Sampling dates (in 2023) for CTD measurements (10 m) and water sampling for Chl *a* and nutrients. Sampling dates for collection of *S. latissima* replicates for both the deployment lines (October 2022 and January 2023) are given.

2.1.2 Water sampling for Chl *a* and nutrients

Water samples were collected at the station inside the farm for [Chl *a*] in-vitro and dissolved nutrients concentrations (nitrate + nitrite (herein referred to as NO_3^-) and ammonium (NH_4^+) on the same dates when in situ CTD measurements were taken. Water samples were taken with a water sampler (5L) at the seaweed cultivation depth (approximately 3m) and transferred to brown acid-washed bottles (8L).

Within a few hours after the water and specimens of *S. latissima* collection, samples for nutrients were filtered in the lab at TBS. A polycarbonate filter (0.8 μm) was used and the filter was flushed before filtering to remove the artificial ammonium in the filter. Then, the filtrate was directly placed in a centrifuge tube and frozen at -20°C, where nutrient concentrations were later analysed in the laboratory. Samples for [Chl $a_{in-vitro}$] biomass were filtered (250 ml - 500 ml seawater, depending on the biomass) with a Whatman GF/F glass fiber filter. Every filter (triplicate) per sampling day was folded, wrapped in aluminium foil and stored in the freezer at -80°C.

2.1.3 Sensor data, wind and light

A C3 submersible fluorometer sensor (Turner Designs, USA) was deployed at a 3m depth at the edge of the farm, close to the MI station (figure 2.1.1 c). This in situ sensor collected Chl *a* fluorescence (later calibrated to mg m^{-3}), turbidity (relative fluorescence unit that was later calibrated to Formazin Turbidity Unit, FTU) and temperature (°C) every ten minutes during almost the whole sampling season. The sensor was equipped with an antifouling copper plate and a mechanical wiper that rotated and cleaned the optical sensor before each measurement was taken.

Furthermore, a HOBO pendant temperature and light logger (HOBO, USA) was placed approximately 200 meters outside the farm that measured light intensity (lux) in the air every 30 minutes for part of the sampling period. Light intensity values were integrated daily according to the Riemann sum and the sum was divided by the total measurement of one day (48) to get a daily average. The values were converted to irradiance, E, of the photosynthetic active radiance region (PAR, spectral window is 400 - 700 nm) (μmol photons m^{-2} s^{-1}). The conversion factor used is 1 kilolux = 16 μmol photons m^{-2} s^{-1} based on Saukshaug et al. (2009).

Wind speed (m s^{-1}) data were collected from the Norwegian Centre for Climate Services from the Sula meteorological station located in the western part of Frohavet (Norwegian Centre for Climate Services).

2.1.4 Lab analysis

A few months after the sampling, the frozen filters for [Chl *a*] in-vitro were extracted with methanol for fluorometric analysis in the laboratory at TBS. Fluorescence was measured with the Turner Design Trilogy fluorometer (Turner Designs, model: 7200-046) and the in-vitro concentration of Chl *a* was calculated by the following equation:

$$\mu g \quad [\text{Chl} \quad a] \quad L^{-1} = \frac{(F - B) * f * E * 1000}{V * 1000} \tag{2.1}$$

Where: F = fluorescence Chl *a* measured, B = blank measurement of 100% methanol, f = 0.47 the calibration factor, E = 5 the extraction volume (ml), and V = volume of filtration (ml).

The frozen filtered seawater samples were used for nutrient analysis, and all nutrients were analysed at TBS. [NO_3^-] was analysed according to the Norwegian standards (NS4745) and [NH_4^+] according to Kérouel and Aminot (1997).

2.2 Bryozoan Coverage Estimation

2.2.1 Image scanning of the lamina

To get highly-resolved images of the kelp lamina, the Canon flatbed scanner LiDE 400 with a scan resolution of 1200 DPI (= 47.24 Dots per mm) was used. This flatbed scanner is a contact image sensor (CIS) type scanner that consists of an illumination part, an optical system and a light-sensing part. This type of scanner has a higher optical resolution, is lower in price and is mostly more compact compared with a charged coupled device (CCD) type of scanner and, thus, easier to work with (Vaughan, 2020). Adhesive measurement tape was attached to the inside of the scanner to get a scale bar in centimetres on every scanned image (figure 2.2.2a). Scans were made with the Canon IJ Scan Utility software and the function Scan Gear. The DPI was set to 1200 to create an image of the lamina that was detailed enough to detect the small bryozoan colonies, larvae and ancestrula (minimum size diameter of 300 μm). The files were stored as a TIFF file to maintain quality and were later processed into SVG files with a program developed by Artur Zolich (Pers comm, 2023). No other settings, such as light and contrast were adjusted.

Frozen specimens of *S. latissima* were thawed before scanning. The sporophyte length (from holdfast to tip of the lamina, herein referred to as just lamina) and width were measured and each was cut into small parts so that the pieces fit on the scanner. The parts were divided into new, mid and old tissue (figure 2.2.1) and lamina pieces were scanned on both sides. Every lamina piece was, at first, gently dried with paper towels to remove excess water, given that too much water made the scanned image blurry. After scanning one piece, the scanner was cleaned with a damp microfiber cloth and a dry cloth.

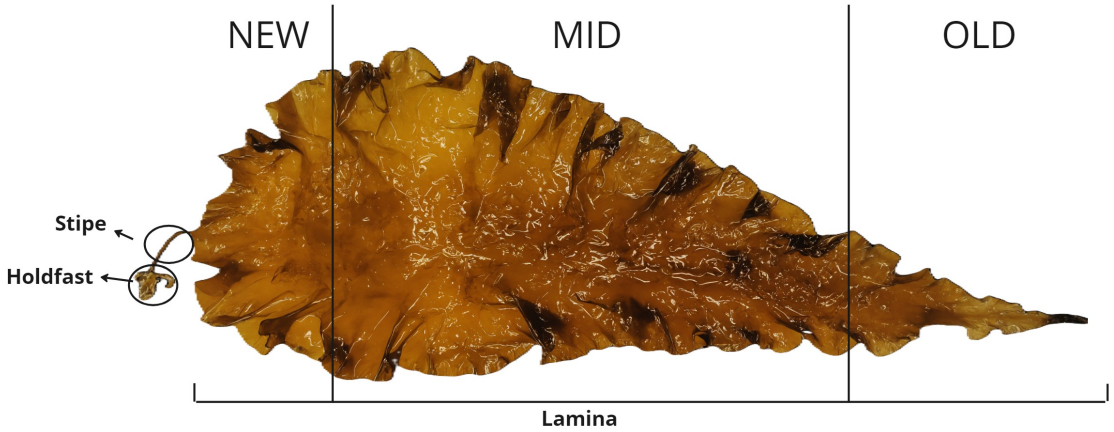

Figure 2.2.1: The kelp lamina divided into a NEW, MID and OLD part and identification of the stipe and holdfast.

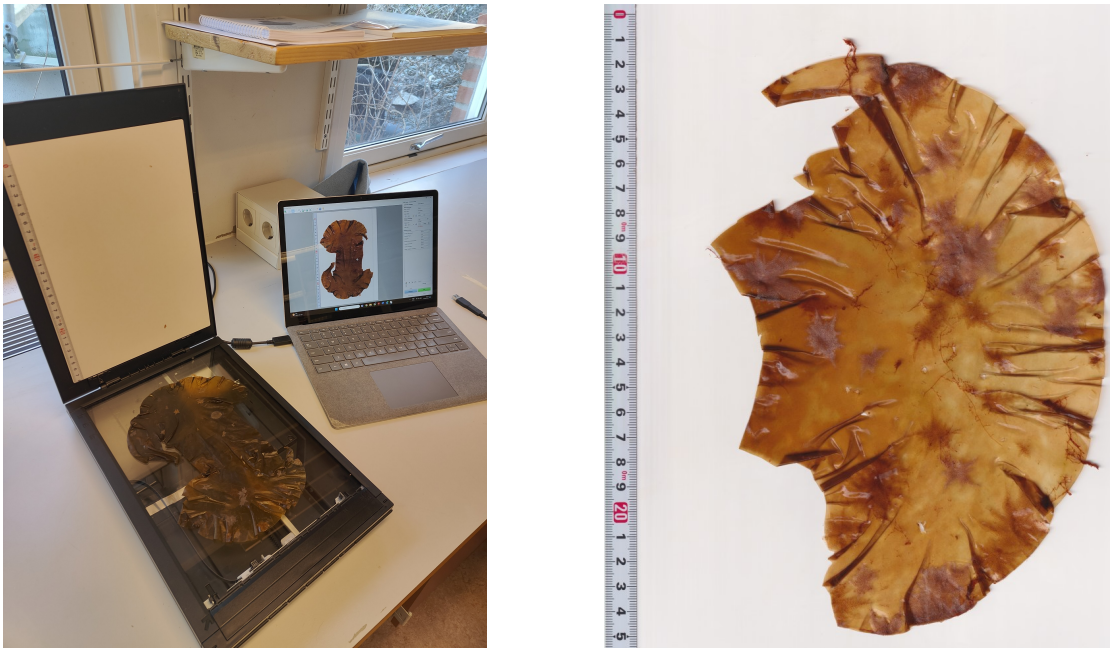

(a) **(b)**

Figure 2.2.2: The Canon A4 flatbed scanner LiDE 400 with kelp (a) and one example of an image with scale bar after scanning (b)

2.2.2 Image analysis

A total of 1037 image scans were made from 63 specimens, including both sides of the lamina. Bryozoan colonies, larval settlement and pre-ancestrulae on the images were manually marked with circles in the vector graphics editor program Inkscape (Inkscape Project, 2020). To shorten the time of manual detection of bryozoans on the images, and because the specimen was sometimes transparent enough to see both sides on one image, only the scanned images from one side of the lamina were used. Exceptions were made to this, based on the logic of the flow chart in figure 2.2.3. In case one side of the lamina contained more than 16 images in total, a subsample of the total images was taken containing four images of the newest (NEW) part of the lamina, four of the middle (MID) and four of the oldest (OLD) part of the lamina (figure 2.2.1). In case the lamina was too dark to see both sides, images from both sides were analysed in Inkscape.

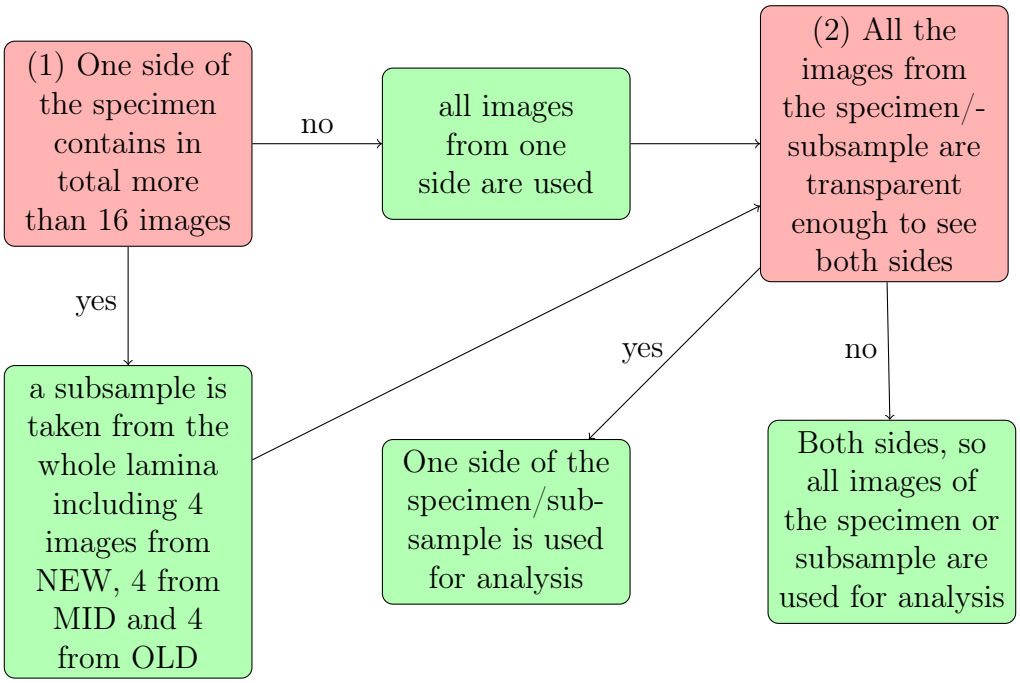

Figure 2.2.3: A flow chart of decision making for image analysis. If one side of the specimen contains more than 16 images, a subsample is taken. If the lamina is transparent enough to see colonies, settled larvae and pre-ancestrulae from the other side as well, only one side is used for analysis.

Bryozoan colonies, larval settlement and pre-ancestrulae were marked by drawing circles around the species. Different colours of circles in Inkscape were used to determine whether a circle was 1) a colony or, 2) a settled larva or a pre-ancestrula. A specimen on the image was identified as a settled larva or a pre-ancestrula if it was a cyphonaute larva that clearly showed a triangular shape of the valves. The larvae mostly have a clear transparent grey/white colour or darker red when it is on the other side of the scanned lamina (figure 2.2.4). The triangular valve can also already be dissolved, but metamorphosis has not been completed yet because it does not show a clear septum yet, a clear ancestrula (pre-ancestrula). Identification of the septum was based on images and explanation of Stricker (1989). Bryozoan colonies were only selected if there was a clear colonization or a sharp red dot that indicates the ancestrula (figure 2.2.5).

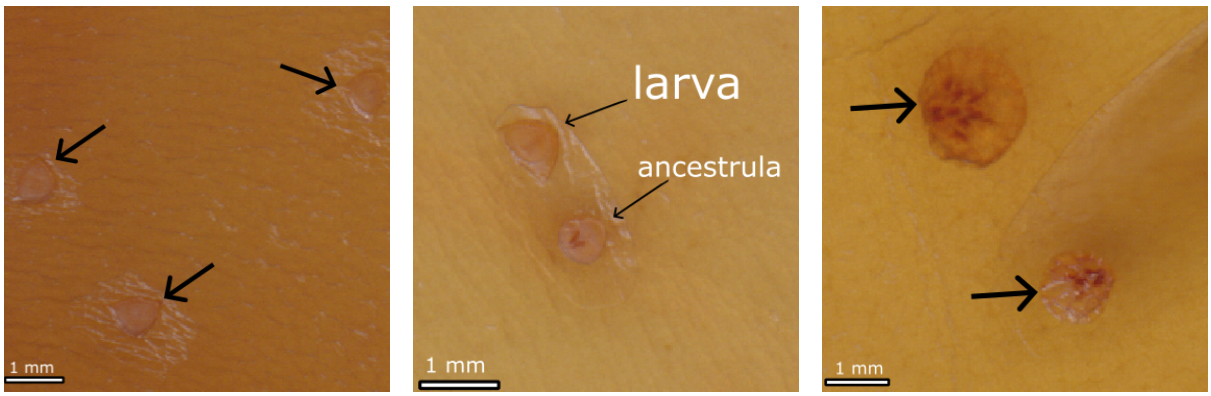

Figure 2.2.4: Three images (close-ups) of the lamina from the line deployed in October 2022 on sample date 15-06-2023. On the left side, three cyphonaute larvae are shown that clearly show a triangular shape. In the middle is another larvae together with a small developed colony where the septum is developed (clearly two red dots are visible). The right image shows bryozoan colonies from both sides of the lamina (the upper left is on the other side).

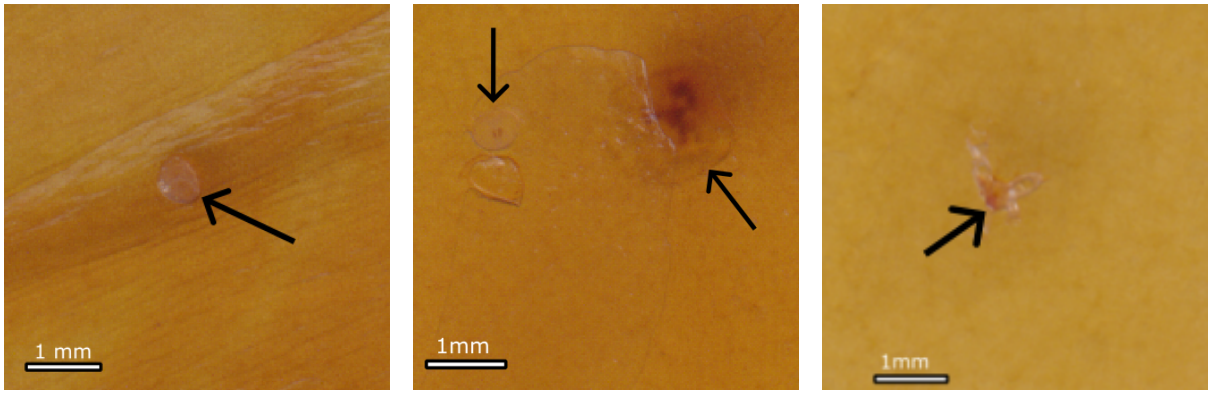

Figure 2.2.5: Three images (close-ups) of the lamina from the line deployed in January 2023. The left image shows one pre-ancestrula. The middle image shows one larva whose valve has been removed but is still visible on the lamina, together with a colony on the other side of the lamina. Both are from sample date 15-06-2023. The right image shows a small just developed colony from sample date 15-05-2023.

2.2.3 Bryozoan coverage percentage, counts and size

The pixel size of the projected lamina area and the marked area were calculated in the programming language Python™ (Latest version used: 3.12.3, Van Rossum and Drake Jr, 1955), and the bryozoan coverage percentage was calculated by the following equation:

$$Percentage\ coverage \quad (\%) = \frac{Marked\ Area}{Projected\ lamina\ area} * 100 \tag{2.2}$$

Here, the marked area (circles that are drawn around bryozoan colonies, settled larvae and pre-ancestrulae), and the projected lamina area are both in pixel size. The projected lamina area was retrieved by using the openCV library in Python (Bradski, 2000), where every scanned image was converted into grayscale and a threshold was made to create a binary mask so pixels of the lamina could be counted. The approximate number of the 'false-positive' pixels from the adhesive measurement tape from the scanner on the images was retrieved by scanning an image of the full length of the scan bed but without any kelp. If both sides of the lamina were marked from one side, the projected lamina area was multiplied by two. Counts of the bryozoan colonies, settled larvae and pre-ancestrulae were also retrieved using Python, where every circle drawn in Inkscape was counted as one. For normalizing the data, the total counts were divided into the total projected lamina surface area and calculated to counts per squared meter lamina area. The size (area) of one projected colony, settler or pre-ancestrula was calculated by the following equation:

$$Circle\ area \quad (\mathrm{mm}^2) = \frac{\pi * horizontal\ r * vertical\ r}{1200^2/25.4^2} \tag{2.3}$$

In this equation, r is the radii of the minor/major half axes of the circle/oval, 1200 is the DPI and 25.4 mm is equivalent to one inch.

The link to the full code for the calculation of the marked area, the projected lamina area, percentage coverage and circle area can be found in Appendix A, as well as the libraries used for retrieving the results.

2.3 Statistical Analysis

All graphic visualisations of the results were performed in Python (Latest version used: 3.12.3, Van Rossum and Drake Jr, 1955), and libraries used for graphic visualisation were Matplotlib, Pandas, Numpy, Seaborn, Plotly and Datetime (Plotly Technologies Inc., 2015; Hunter, 2007; McKinney and & Others, 2010; Harris et al., 2020; Waskom, 2021).

Statistical analysis was conducted using the software programming language for statistical computing graphics R, version 3.3.0+ (R Core Team, 2024), through RStudio™ version 2023.12.1+402 (RStudio Team, 2020). The data used for statistical analysis can be found in Appendix B. Correlation matrices were performed with the *corrplot* function in R. Non-parametric, pair-wise Spearman correlation was used to calculate the correlation coefficients and the statistical significance ($p < 0.05$) between the environmental data and the bryozoan data. An average of four days before every sampling date was calculated for temperature, Chl *a*, and turbidity. Four days are used to take into account the approximate metamorphosis time of the settled larva (Zimmer and Woollacott, 1977).

To examine the effect of temperature and Chl *a* on the bryozoan coverage data, including the effect of time, the cumulative values of temperature and Chl *a* were calculated from the sensor data. For every period in between the sampling dates, the measurements of temperature and Chl *a* were summed up (Riemann Sum). The sum was divided by the total measurements per day (144) to get the cumulative temperature and Chl *a* for every period. The missing days in the data set (25/04/2023 - 07:20 to 27/04/2023 - 09:20, missing 302 measurements in total) due to battery change of the sensor were calculated manually by taking the last and first degrees measurements in between this gap of missing days (6.39 °C and 6.69 °C). The same was done for the Chl *a* (1.08 mg/m^3).

The averages of the replicates for each date for both deployment lines were used for statistical analysis. To include time, delta coverage percentage and delta colony counts were used (= subtracting the value of percentage coverage or counts from the previous sampling date from the value of percentage coverage or counts from the next sampling date). To examine the effect of the cumulative temperature, cumulative Chl *a* and deployment line on the difference in bryozoan coverage with respect to every previous sample date, a beta regression model was used as the bryozoan coverage data is in percentages (Smithson and Verkuilen, 2006). For the abundance, a generalised linear model (GLM) was used with Poisson distribution as the colony abundance data is counting data. Nutrients were not included in the model because of the lack of data for two sampling dates (the 15^{th} of May and the 15^{th} of June). Irradiance (E_{PAR}) was also not included because of not enough data points to compare.

key environmental variable	**data points to compare**	**used in statistical model**
temperature (°C)	5	cumulative
Chl *a* (mg m^{-3})	5	cumulative
turbidity (FTU)	5	no
NO_3^- (μM)	4	no
NH_4^+ (μM)	4	no
average daily E_{PAR} (μmol photons m^{-2} s^{-1})	3	no
line	5	factor (2 levels)

Table 2.3.1: Predictor variables available for modelling

Chapter 3

Results

3.1 Environmental data

In general, time series data (every ten minutes, figure 3.1.1) from the C3 submersible sensor show that temperature was below 6 °C from mid-February until the beginning of April, dropping slightly in mid-March (approximately 5.5 °C) but increased steadily from April until the end of June (from 5 °C to approximately 12 °C). Turbidity peaked at the beginning of March (up to 0.4 FTU) and at the end of April (up to 0.2 FTU), gradually increased from May to June ($>$ 0.2 FTU in June) and dropped by the end of June. Chl *a* rapidly increased at the beginning of April (up to 6 mg m^{-3}), reflecting the occurrence of the spring bloom and fluctuated around 2 mg m^{-3} over the rest of the sampling period (Volent et al., 2011).

Integrated 24-hour irradiance (E_{PAR}) above the water showed some peaks during the whole period in average values up to 400 µmol photons m^{-2} s^{-1} (figure 3.1.1e). At the beginning of May, there was some period of high average daily irradiance (peak up to 400 μmol photons m^{-2} s^{-1}) together with low wind speed (below 5 m s^{-1}), suggesting a period with clear skies. At the end of May, the wind speed was strong (up to 20 m s^{-1}), and the average E_{PAR} per day was low (down to 100 μmol photons m^{-2} s^{-1}), reflecting the occurrence of a storm (figure 3.1.1d and e).

Vertical depth profile measurements showed a clear increase in temperature from April towards the end of June, with earlier days (April) and the 7^{th} of June showing a well-mixed water column (figure 3.1.2a). Stratification started from the 10^{th} of May, except on the 7^{th} of June, the waters were well mixed. The water column became stratified again on the 29^{th} of June. Salinity varied in time (from 34.2 to $<$33) with the lowest salinity levels on the 29^{th} of June and the 5^{th} of May (figure 3.1.2b). Turbidity explains how much light is backscattered, which can be particles or air bubbles in the water, and Chl *a* represents how much phytoplankton there is in the water column, thus how much food is available for bryozoan to eat. The highest Chl *a* and turbidity measurements were obtained in May (7 µgL^{-1} and 0.8 FTU), but it should be taken into account that there were no measurements of Chl *a* and turbidity at the beginning of the sampling period due to malfunctioning of the CTD (figure 3.1.2c and d).

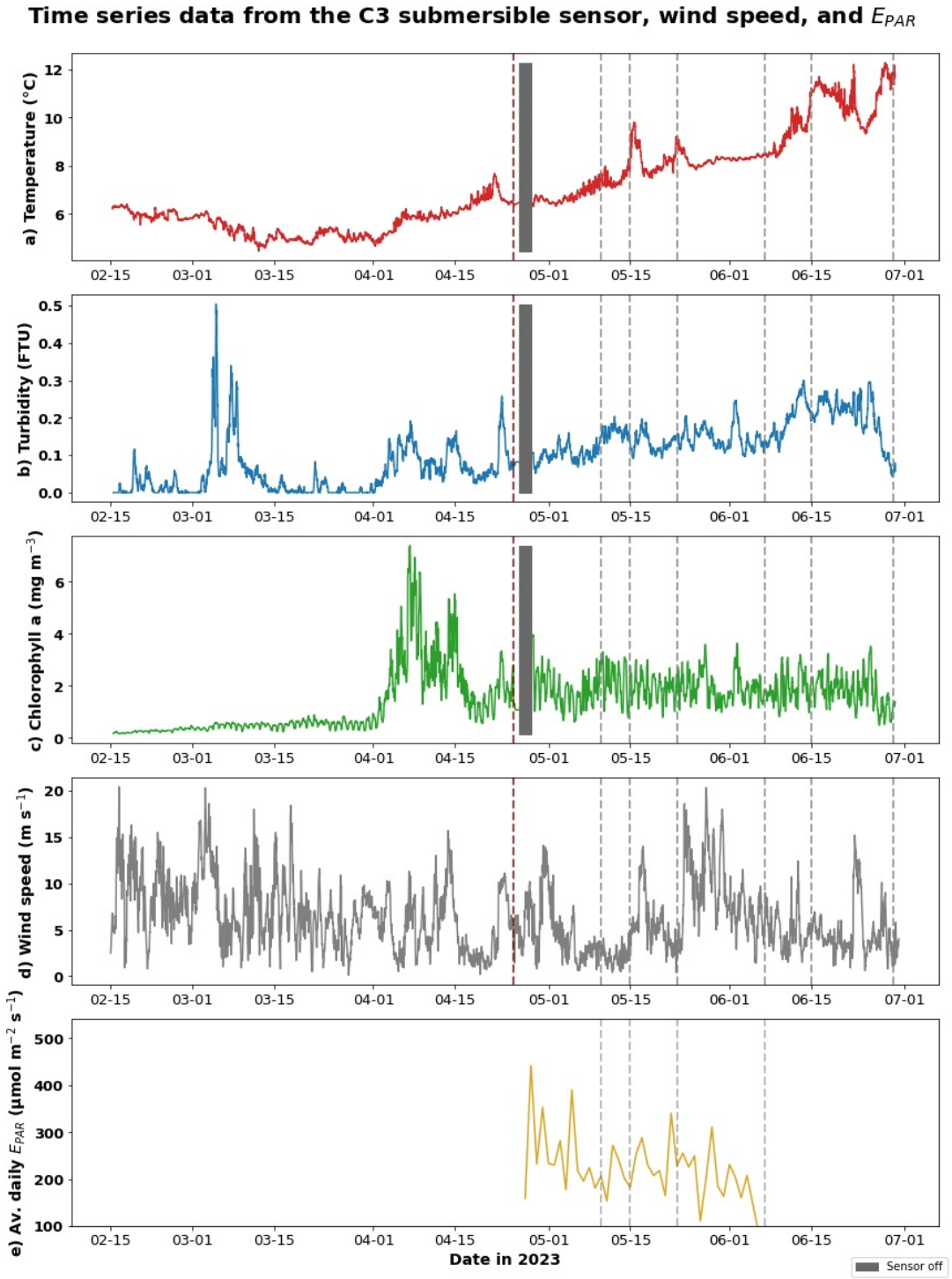

Figure 3.1.1: Time series (every ten minutes) data showing a) temperature (°C, red), b) turbidity (FTU, blue), and c) [Chl *a*] (mg m^{-3}, green) over the whole sampling period (mid-Feb until late June) from the C3 Submersible sensor at 3m depth at MI station. d) Time series data of the wind speed (m s^{-1}, grey, every 1 hour) at the Sula station for the whole sampling period retrieved from Seklima.met.no and e) showing the average E_{PAR} per day (yellow) for part of the sampling period (end of April until the beginning of June). The grey dotted lines indicate the sampling dates of kelp collection for bryozoan coverage estimations. The red dotted line indicated that only sampling for the October line was done. The grey boxes indicate the lack of data because of battery change.

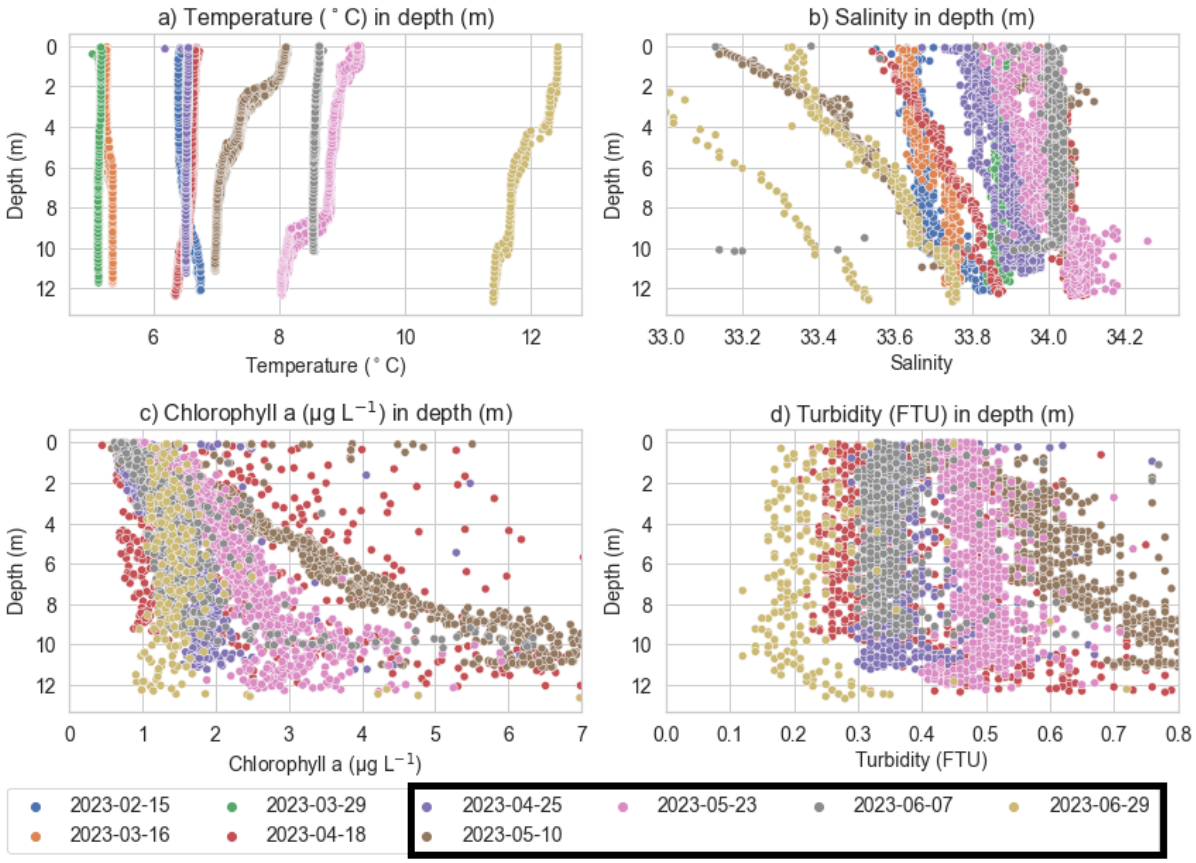

Figure 3.1.2: Vertical depth profile measurements from the edge of the farm (MI station) for a) temperature (°C), b) salinity, c) chlorophyll *a* (μg L^{-1}) and d) turbidity (FTU). Due to malfunctioning of the CTD, information about Chl *a* and turbidity is only obtained from April until the end of June. The dates in the black box indicate the dates when the sampling of kelp replicates was also done.

3.2 Chl *a* and nutrient concentration

[Chl *a*] in vitro measurements show the same pattern compared with the CTD data and show a gradual increase in Chl *a* (μg L^{-1}) in time with a peak on the 10^{th} of May ($>$ 5 μg L^{-1}), and a decrease after that (figure 3.2.1b). On the 6^{th} of June, values were high (from 6-8 μg L^{-1}). NO_3^- concentrations sharply dropped after the 29^{th} of March from 5.5 μM to 0.5 μM right before the occurrence of the spring bloom at the beginning of April (figure 3.2.1d). NH_4^+ concentrations dropped in March until the 18^{th} of April (0.05 μM) and dropped again on the 10^{th} of May (figure 3.2.1c).

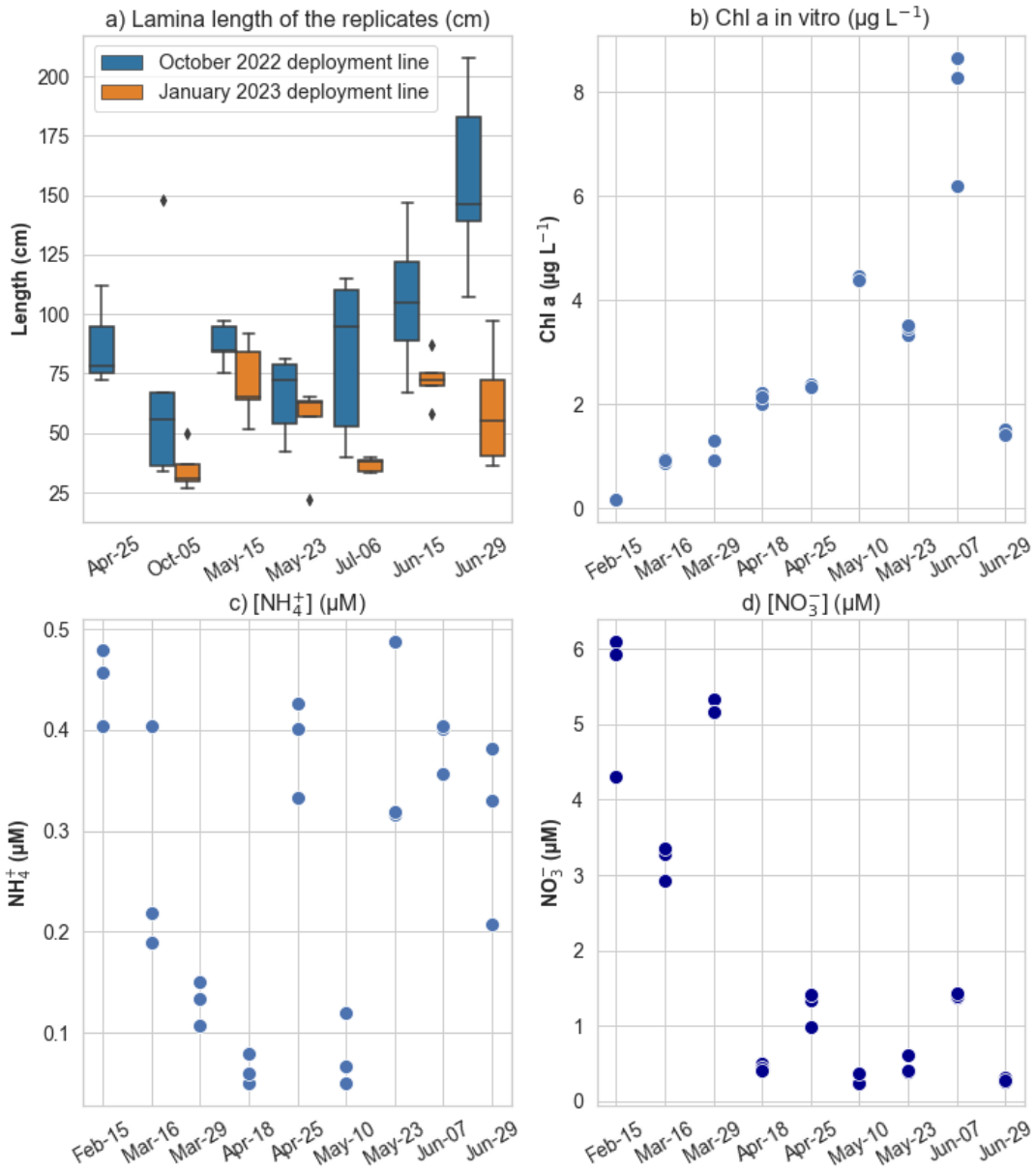

Figure 3.2.1: A figure of a) the lamina length of the replicates taken from the deployment lines that were used for bryozoan quantification, b) [Chl *a*] in vitro measurements, c) [NH_4^+] measurements, and d) [NO_3^-] measurements. For the nutrients and Chl *a* triplicates were taken for each date at the MI station.

3.3 Bryozoan coverage

Samples were collected to register bryozoan coverage on *S. latissima*. Based on weather circumstances and the farmers' availability, seven different sample dates were used. Samples were taken randomly from the research line (10m, at MI Station).

The first settlement was detected on the 25^{th} of April with a total of six settled larvae from all the samples taken that day. No clear colonies were detected, and the lamina contained many transparent features that initially appeared to be bryozoan colonies but were later confirmed to be snail eggs under the microscope. Samples from this same date contained many spots that resembled pre-ancestrulae, but it was too small/vague to determine. This also applied to the samples taken in early May. However, samples from the 10^{th} of May clearly showed the first settlement, metamorphosis and colony formation on the images.

S. latissima from both deployment lines had almost zero percentage bryozoan coverage for the first four sample dates (April to May, figure 3.3.1a). However, percentage coverage rapidly increased in the middle of June with a higher percentage of coverage for the October deployment line (average of 11% coverage) compared with January (average of 3% coverage) on the 29^{th} of June. The total counts of colonies per m^2 *S. latissima* increased gradually/linearly and showed the same pattern for both deployment lines with the highest number of colonies on the 29^{th} of June (approximately 1260 counts per m^2 for October and 860 for January, figure 3.3.1b).

Two peaks in the total settlement and pre-ancestrulae counts occurred for both lines on the 15^{th} of May and the 15^{th} of June (187 and 826 counts per m^2 for October, respectively and 126 and 618 per m^2 for January). Almost all of the settlement and pre-ancestrulae were found on the meristem, the newer part of the lamina, for the whole sampling period. For June, bigger colonies were found particularly at the older part (tip) of the lamina.

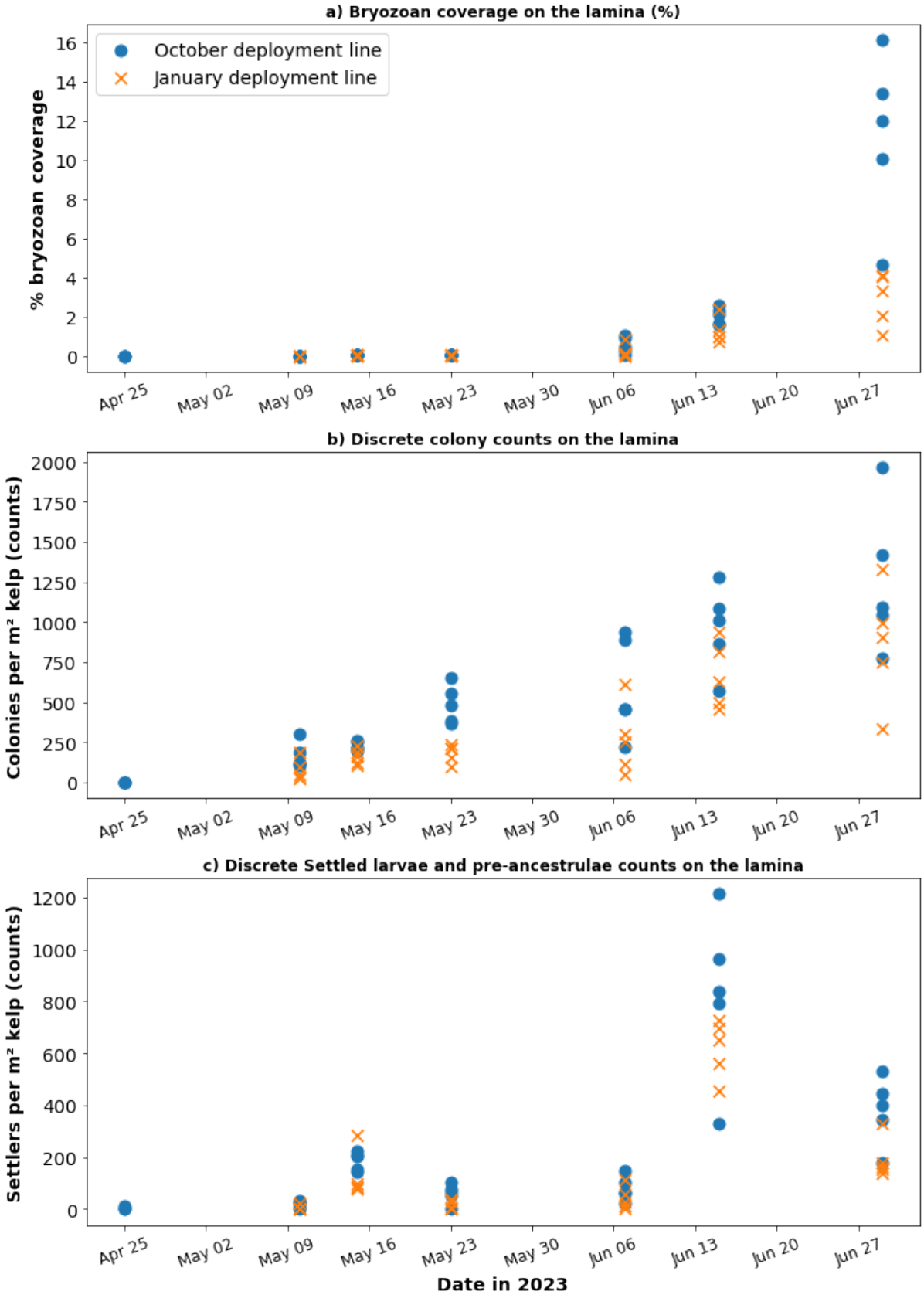

Figure 3.3.1: Graphs showing the a) bryozoan percentage coverage from the total project lamina area, b) counts of colonies and c) larval settlement and pre-ancestrulae per m^2 kelp for samples of the October deployment line (blue) and the January deployment line (orange) in time.

Overall an average percentage coverage of 3% and 11% sounds quite low. However, images showed that, by the end of June, the kelp was already heavily fouled, which compromised the quality of the product. Low percentage coverages in June were already completely covered with many small colonies (figure 3.3.2).

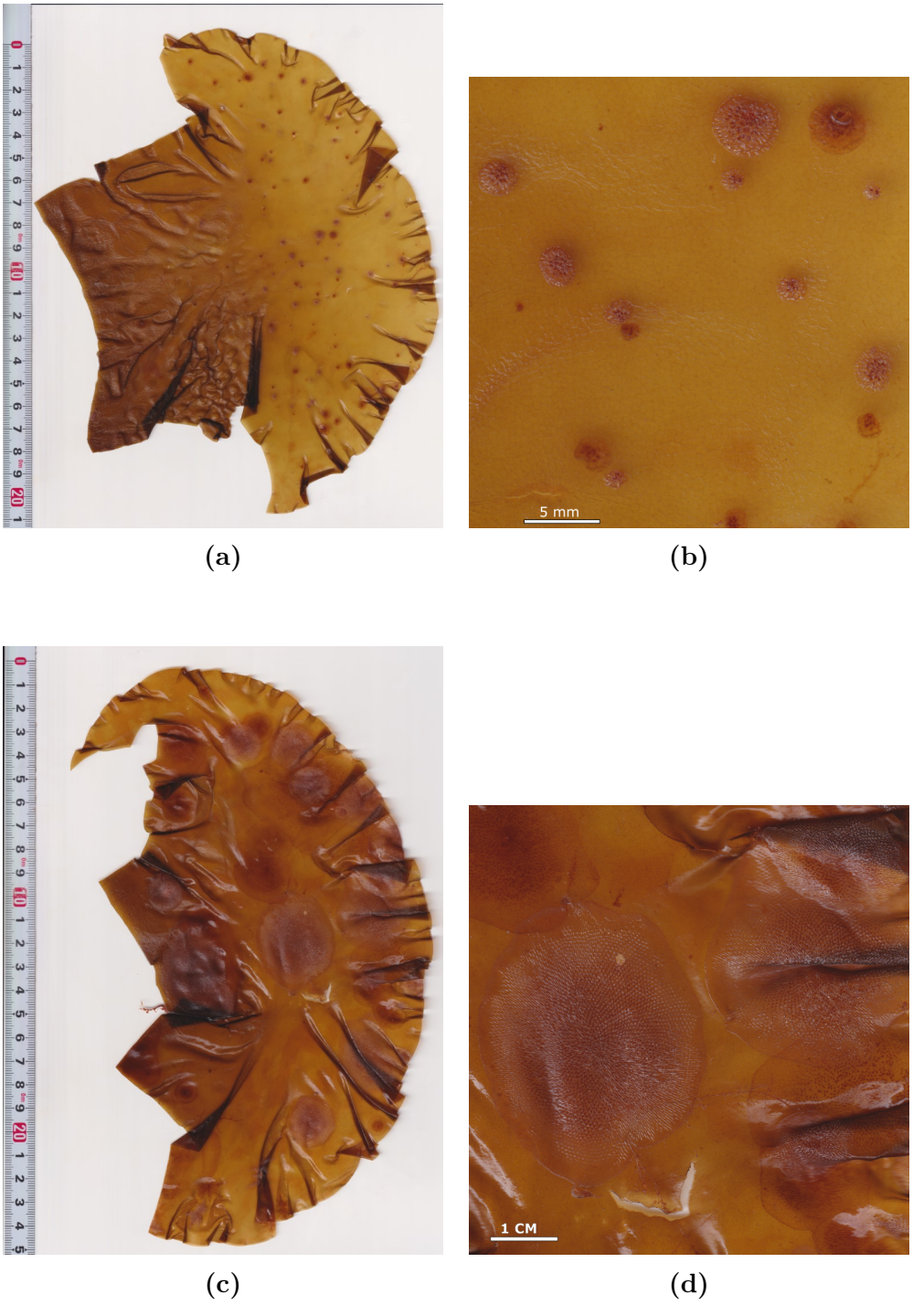

(a) **(b)**

(c) **(d)**

Figure 3.3.2: Examples of scanned images of the lamina with different percentage coverage from the October 2022 deployment line. a) shows a scanned lamina piece with a coverage of 1.5% of which the whole replicate had a coverage of 13.4%. b) is a close-up of a. c) shows a scanned lamina piece with a coverage of 33.1% of which the whole replicate had a coverage of 13.4%. d) is a close-up of c.

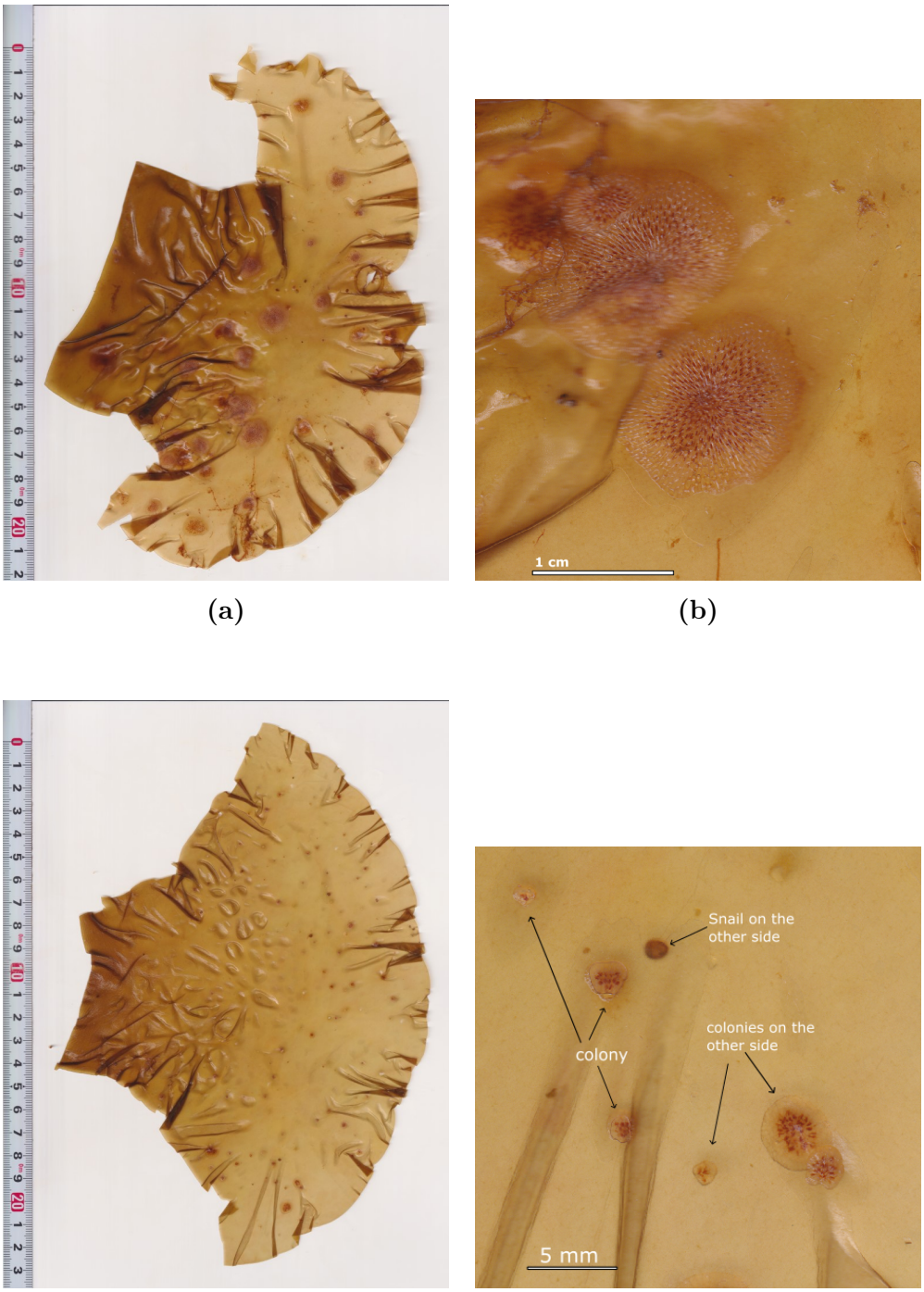

(a) **(b)**

(c) **(d)**

Figure 3.3.3: Examples of scanned images of the lamina with different percentage coverage from the January 2023 deployment line. a) shows a scanned lamina piece with a coverage of 6.64% of which the whole replicate had a coverage of 4.08%. b) is a close-up of a. c) shows a scanned lamina piece with a coverage of 0.5% of which the whole replicate had a coverage of 4.08%. d) is a close-up of c.

3.4 Bryozoan colony and larval settlement size

In total, 13307 colonies, settled larvae and pre-ancestrulae were detected on the scanned images, from which 3803 counts were from the replicates from the line deployed in January 2023 and 9504 counts from the line deployed in October 2022. The circle size area around the species was calculated and results of the bryozoan colony size and abundance are shown in figure 3.4.1. The results show that with an increase in time, bigger colonies (< 2 mm^2 in log + 1) were detected. The increase in colony size showed almost a linear trend on the log scale. The largest colonies (between 3 to 4 mm^2 in log + 1) were only found on the 29^{th} of June with the lowest abundance. The highest abundance of colony sizes was found in the smallest range (0 - 0.5 mm^2 in log + 1) for this date as well.

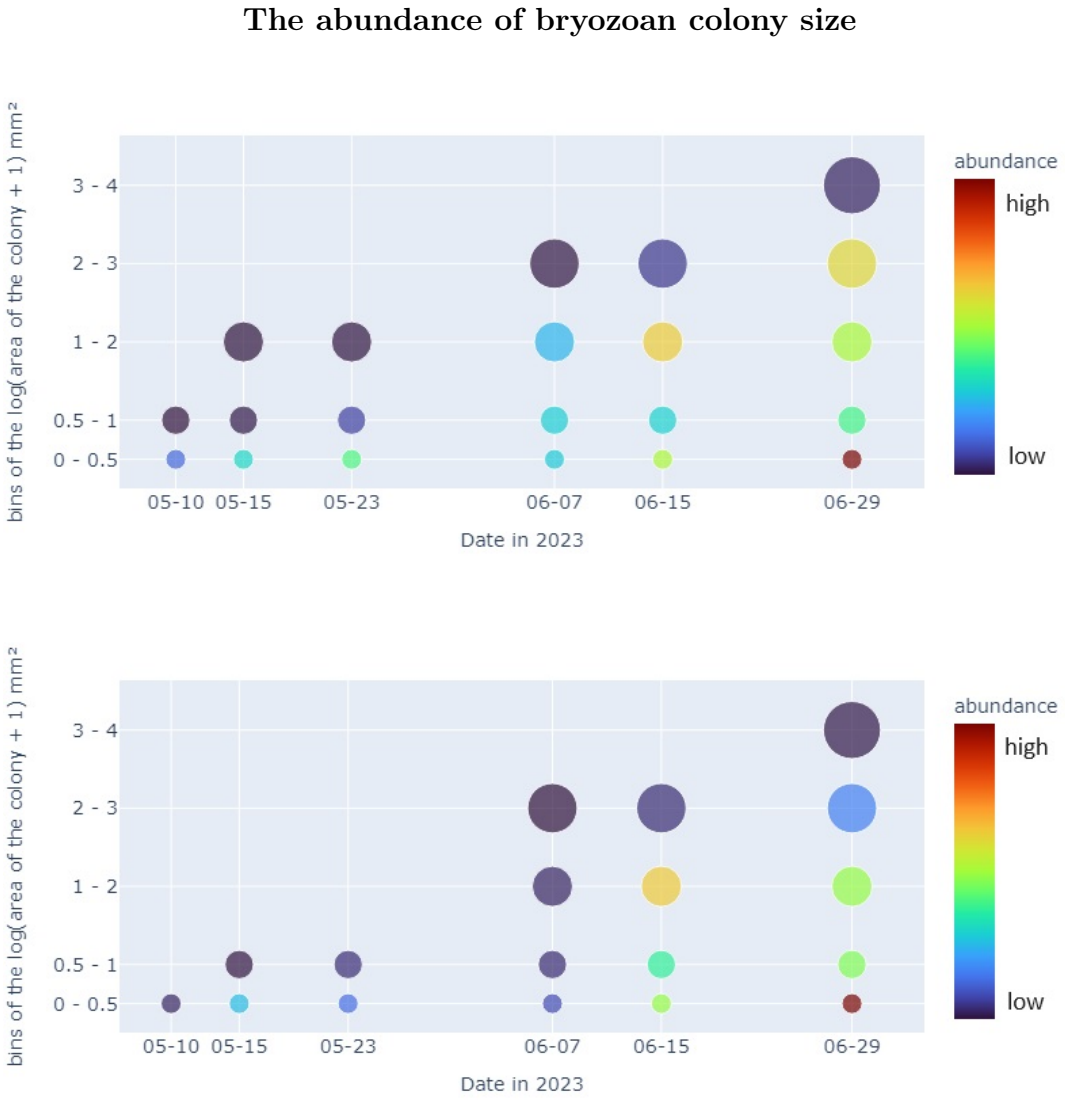

Figure 3.4.1: The total abundance of bryozoan colony size for the different dates for a) the October 2022 deployment line and b) the January 2023 deployment line. The Y-axis and circle size indicate size ranges in log(area + 1) mm^2. The different colours in Z indicate the abundance including all observations (counts), with high counts in red and low counts in darker blue, meaning that the abundance is relative to total observations.

The size of settled larvae and pre-ancestrulae seems to increase in time, with an equivalent spherical diameter between 0.4 mm and 0.6 mm for May and the beginning of June (figure 3.4.2). There was some variation for these dates with higher values up to 0.9 mm. A higher abundance of settled larvae and pre-ancestrulae was observed for the last two dates, the 15^{th} of June and the 29^{th} of June. The size showed a peak between 0.6 and 0.7 mm.

The abundance of the settled larvae and pre-ancestrulae size (ESD in mm) for the different dates

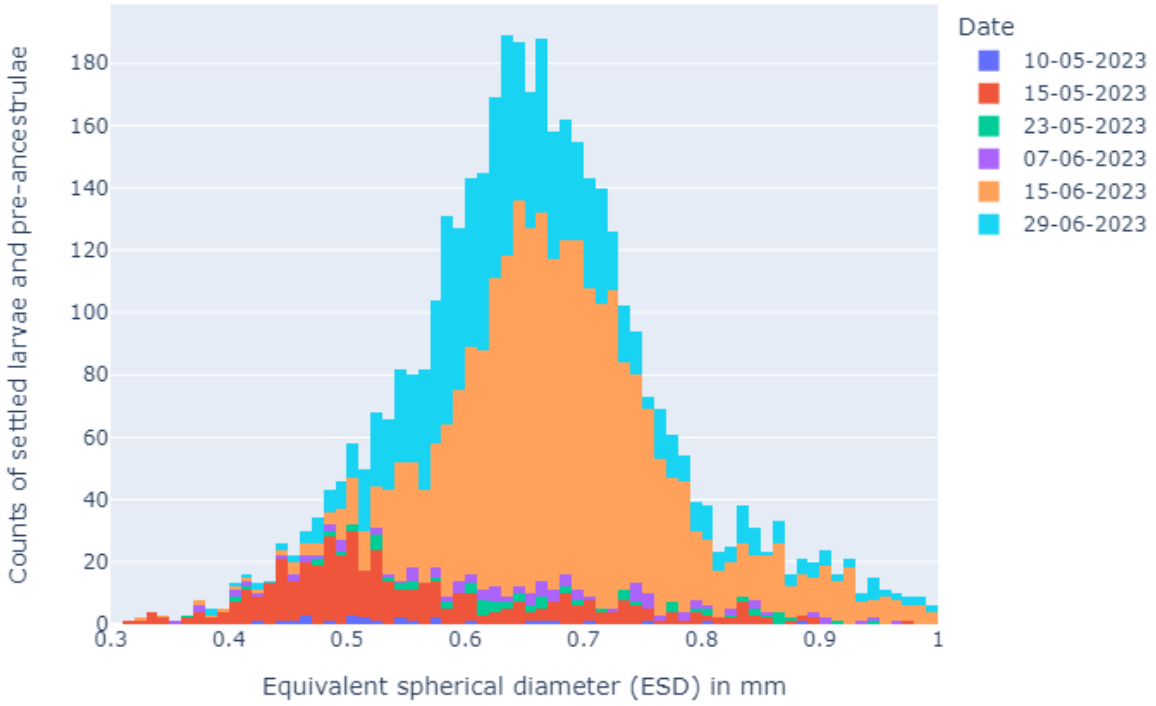

Figure 3.4.2: A histogram of the abundance of the settled larvae and pre-ancestrulae size for the different dates. The size is calculated to the equivalent spherical diameter (ESD, mm).

3.5 Environmental variables effect on bryozoan coverage

3.5.1 Spearman's rank-order correlation

To investigate correlations between the environmental variables and bryozoan coverage of the different deployment times, correlation matrices were performed. Spearman's rank-order correlation showed patterns of correlation between the average temperature, Chl *a*, and bryozoan data. The average temperature shows a positive correlation for both deployment lines with colony counts (0.89 for October and 0.82 for January $p < 0.05$) and the percentage coverage (0.94 and 0.89 respectively, $p < 0.05$). The average turbidity has no significant correlation (-0.08 and -0.01, $p < 0.05$) with the bryozoan coverage, and for Chl *a* the correlation is negative (-0.53 and -0.41, $p < 0.05$).

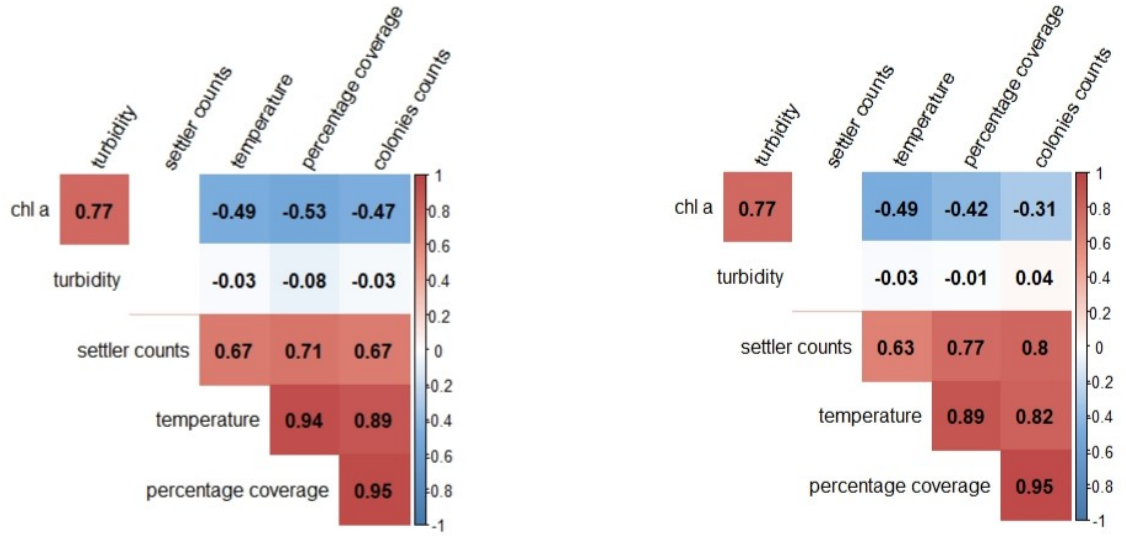

Figure 3.5.1: Spearman correlation plot of the average temperature, turbidity and chlorophyll *a* and the bryozoan colony and settled larvae and pre-ancestrulae (settlers) counts and percentage coverage data from a) line deployed in October 2022 and b) line deployed in January 2023. Statistically significant ($p > 0.05$) positive correlations are shown in red and negative in blue. White empty boxes indicate the correlation between the two variables was not significant ($p > 0.05$).

3.5.2 Temperature, Chl *a*, and deployment line effect

The model selection indicated that the optimal model for bryozoan percentage coverage with respect to every previous sample date included cumulative temperature, Chl *a* and the deployment line (table 3.5.1). All interactions gave no significant effect ($p > 0.05$). One degree×day increase in the temperature would lead to a 0.07 (± 0.01, $p < 0.05$) increase in the log odds of fraction coverage. There is a significant negative effect of the cumulative Chl *a* on the fraction coverage (table 3.5.1). As the total sample dates are small, with a big-time interval in June (14 days), the data does not properly fit the model. Cook's distance is large as it treats the bigger values of the fraction coverage as outliers. The same accounts for the model selection for the colony abundance with respect to every previous sample date. This model also included all environmental variables as the optimal model. However, the dispersion parameter is very high (approximately 91) indicating that there is more variability than expected. This is obviously due to the great time step in June (and the small sample size), as changing the model in link or type did not make a difference.

Model	Response variable	Predictor variables	Model results			Model assessment
			Estimate ± SE	Test-statistic	p-value	
Beta regression 1	Delta coverage fraction	Cumulative temperature	0.07±0.01	6.52	7.03e−11	Pseudo R2 = 63%
		Cumulative Chl *a*	-0.32±0.08	-4.03	5.62e−5	
		Line	1.24±0.36	3.47	5.26e−4	
Beta regression 2	Delta coverage fraction	Cumulative temperature	0.05±0.01	3.81	1.4e−4	Pseudo R2 = 69%
		Cumulative Chl *a*	-0.21±0.09	-2.41	1.613e−2	
Beta regression 3 (only temperature)	Delta coverage fraction	Cumulative temperature	0.02±0.01	2.55	1.07e−2	Pseudo R2 = 44%
GLM Poisson	Delta counts	Cumulative temperature	0.02±0.00	16.14	$< 2e{-}16$	Dispersion parameter: 635.99/7
		Cumulative Chl *a*	-0.13±0.01	-14.88	$< 2e{-}16$	
		Line	0.38±0.05	8.32	$< 2e{-}16$	

Table 3.5.1: Results of the statistical models with response variables fraction coverage (beta regression) and colony counts (GLM, Poisson distribution). Explanatory variables used are cumulative temperature, cumulative chl *a* and the two different deployment lines (October 22 and January 23).

Chapter 4

Discussion

4.1 The method: Image scanning

Studies that explored the quantification of bryozoan coverage have been done before using a simple grid (Matsson et al., 2019), a light table (Førde et al., 2016) or a camera with a UV lamp and image manipulation (Cohen, 2019). In this study, digitalizing bryozoan coverage using a low-cost (< 200 euro) flatbed scanner was applied for the first time. The method in this thesis did not only allow the digitalization of bryozoan colonies but also the first settlement of cyphonaute larvae and pre-ancestrulae (= larvae that are in metamorphosis on the lamina) because of the high resolution that the scanner is able to scan in (1200 DPI). Normally, settlement is difficult to observe with the naked eye and magnification is used. Being able to see larval settlement and pre-ancestrulae is important for early detection and proper quantification of bryozoan growth on the lamina when the seaweed is still suitable for the market. Another advantage is that the setup of the method was easy to handle, as only a scanner and a PC are needed to obtain the images. This makes it user-friendly and cost-effective for seaweed farmers to collect and store information on bryozoan coverage and colony growth in their farms.

Additionally, by using flatbed scanning, the difference in distance between the object and lens and light source is fixed, which improved the consistency of the experiment by constantly having the same settings. The high image resolution (1200 DPI) of the flatbed scanner made it possible to estimate colony size (individual growth) versus larval settlement/colony counts (reproduction), which can bring ecological insights into the growth of old settled colonies versus the recruitment (Yoshioka, 1982). Moreover, this method is also suitable for other fouling, such as Bivalvia, filamentous algae and hydroids, which could be detected as well. This has been shown by Wassick et al. (2023), who measured the recruitment and growth of biofouling communities including tunicates, bryozoan species, algae and many other species on panels. The study also used a simple flatbed scanner but used a higher DPI (2400). In this project, other biofouling species were detected but not taken into account.

Although this method showed great potential in detecting larval settlement, pre-ancestrulae and accurately quantifying bryozoan colonies on the lamina, as a first-time exploring it was time-consuming and labour-intensive. This was because many images had to be retrieved if the kelp lamina was long, particularly in June (for example, the longest replicate was in June with 208 cm in length and had 90 scanned images including

both sides). Also, the lamina needed to be cut into many parts (up to 30) to fit into an A4 format scanner. Because it was so time-consuming, it was not possible to take more than five replicates, which could have affected the high variability in percentage coverage for the later stages. This could be improved by scanning with a larger format (A3, for example, although the scanner would be more expensive) or by having subsamples of the whole lamina from the mid, old and newest parts. This is suitable, as coverage is quite uniform over the whole lamina. In this project, subsamples were taken when there were more than 16 images for one side, but the subsamples were not cut into the same lengthwise zones from stipe to tip. This is important to take into account so the replicates are representative for the sample date. Another challenge was to annotate the colonies, larval settlement and pre-ancestrula by hand in Inkscape, which was a time-consuming task. Giving a rough estimation that colony detection will take up to 15 minutes per image, for example, means that, for the 702 images used in the end (including taking sub-samples), about 176 hours would be used for bryozoan detection. Automation of bryozoan detection would greatly improve the time of data collection and allow for more samples to be collected to give an overview of the bryozoan growth within a farm or from multiple farms from several locations. The initial attempt of machine learning techniques for quantification of bryozoan percentage coverage has already been reported with success (Hassan, 2024), although there was a limitation in small bryozoan segmentation (area less than 0.2 cm by 0.2 cm) which has less Average Precision (AP) results (AP = 41%) compared to large ones (AP= 67%), resulting in a total segmentation of AP bryozoan of 44%.

As this method has never been tried before, several changes can greatly improve the quality of the images and reduce the time of data collection. Table 4.1.1 highlights all factors affecting the results and states suggestions for improving this method. For example, one factor that affected the data was that water reduces the sharpness and contrast in parts of the image and decreased the overall percentage coverage of bryozoans on kelp lamina. Testing different drying methods to remove excess water could improve the image quality and bryozoan detection. Leaving the seaweed hanging to dry for a certain time (with caution so it does not damage the lamina) could be a possibility because this will not affect the fouled organisms on the lamina.

During this project, extra scans were made with different samples (not included in the data) to check whether changing the settings in the IJ scan utility program positively affected the detection of bryozoans in the image. Changing the settings, such as the RBG, DPI and contrast, did not show any differences in bryozoan detection. Besides, the use of a higher DPI and contrast only increased the blurry effect of water and depth differences even more. Changing the DPI, in addition, greatly increased the time of scanning one image. Another possibility is to have a scanner where the light source can be changed and/or to explore scanning with a CDD-based scanner. This is a scanner that tends to have a greater depth of field, which can be useful for objects with high texture (e.g. folding) that create these different depths (Vaughan, 2020).

The innovative part of this method is that it made it possible to detect the first settlement of cyphonaute larvae and larvae that are in metamorphosis on the lamina (pre-ancestrulae). It is known that a competent cyphonaute larva needs to achieve a certain size as a response to its maturation to settle and start its metamorphosis (750 µm in length for *M. membranacea* and 400 µm for *E. pilosa*; Ryland and Stebbing, 1971).

Most observations of the settlement and pre-ancestrulae in this study had a spherical equivalent diameter between 500 and 900 µm within a range of 300 to 1000 µm. This observed size range was quite large compared to the size of cyphonaute larvae and pre-ancestrulae that is observed in other studies and the reason for this can be that no distinction was made between the different stages of metamorphosis. Larvae that just settled still had their valves (pre-metamorphosis) and the pre-ancestrulae mostly had no valve anymore. In that case, it would be better to distinguish these stages to obtain more exact information about their sizes when settled.

Factor	**Error**	**Change**	**Possible solution**
Water	Spectral light attenuation of water reduces sharpness and contrast of the image	Underestimation of percentage coverage and counts	Exploring a time indication for hanging seaweed dry before scanning
Freezing and thawing of the lamina	Some colonies got loose from the lamina when thawing the seaweed	Underestimation of the data	Immediately scan after sample collection (when fresh)
Folding of the lamina	Folding create differences in depth which can reduce sharpness in parts in the image	Underestimation of percentage coverage and counts	Explore the use of a CDD scanner
Settlement and metamorphosis of bryozoans	Metamorphosis has different stages where the transparent valve has already disappeared.	Overestimation of settled larvae, pre-ancestrulae and colony size	Differentiate between species that still have their transparent valve and not (differentiate between pre-metamorphosis, pre-ancestrula and ancestrula)
Other biofouling on the lamina	Many spots were too small to determine whether it was a pre-ancestrula or something different (e.g. snail egg)	Underestimation of pre-ancestrulae and colony counts	Explore scanning with a higher DPI provided that the issue with blurry spots is controlled first
Cutting of the lamina	The lamina was cut into parts to fit on the scanner	Underestimation of colony size	1) Work with an A3 scanner 2) take subsamples of the same length where colonies are not cut

Selecting bryozoans in the Inkscape program with circles	Not all bryozoans are circle-shaped (*E.pilosa* is star-shaped), but all colonies were selected with circles.	Overestimation of the percentage coverage and colony size	Differentiate between different species by using a segmentation program that is able to select the colony only.
Kelp area estimation with grayscale and false positive pixels from the measurement tape	Not all images had the same size (not the whole scan bed was scanned)	Underestimation of the kelp area	1) Always use the full length of the scan bed 2) Explore the opportunities with the Segment Anything Model and its corresponding data set, SA-1B (Kirillov et al., 2023). This was the first method, but it created large errors with segmenting all the kelp. It needs more tuning to fully implement it for this purpose
Uneven scanned kelp lamina parts	Not all pieces had the same length and the kelp was cut into random parts	Error when a subsample is used	Divide the kelp into lengthwise 10 cm zones, from the stipe to the tip (the older part of the lamina) as was done in Denley et al. (2014)

Table 4.1.1: A table of factors with errors given that affected the data quality with either an underestimation or overestimation in the bryozoan quantification data and kelp lamina area estimation. The last column highlights suggestions to reduce or avoid the error of the factor given.

4.2 Environmental effects on larval settlement

In this study, the first bryozoan settlement was observed and detected in the scans on April 25^{th}, when the temperature was around 6.63 °C, while the first colonies (> 1 mm in diameter) were observed at the beginning of May when the temperature was slightly warmer (7.28 °C). The appearance of the first colonies is in line with what farmers expect and a previous study by Njåstad (2018), who observed the first bryozoan colonies at the beginning of May (approximately 7.5 °C) in Skjørafjord, an area as the crow flies 70 km away from Frøya. Matsson et al. (2019) observed the first colonies later in the season, around mid-July, in Northern Norway (Troms, 6 - 8 °C). Førde (2014) observed the first colonies on the 18^{th} of June (approximately 10 °C) in Frøya at the Taraskjæra farm from Seaweed Solutions, which is a bit more exposed than Måsskjæra. This is later in the season and also at a higher temperature. The exact size of the first observed colonies was not mentioned in the study so it could be that the method (camera and light table) used did not detect very small colonies.

In total, two peaks in larval settlement and pre-ancestrulae counts were observed for both deployment lines, one on the 15^{th} of May and one on the 15^{th} of June (187 and 826 counts per m^{-2} for October, respectively and 126 and 618 per m^{-2} for January). This is in contrast with Saunders and Metaxas (2007), who observed an exponential increase in time in settlement of *M. membranacea* in Nova Scotia, Canada, between May and July, rather than peaks in settlement. For both peaks, the samples were collected in a period where there was a sharp increase in temperature from 7 °C to around 9 °C for the first peak and 9.5 °C to 11.5 °C in the second peak. This indicates that a high cumulative temperature (a higher rate of increase in temperature) could positively influence the rate of settlement. M. Saunders and Metaxas (2007) showed that the growing degree day (= cumulative temperature) explained 81% of the variability in settlement abundance. Apart from that, there was a period with high wind speed (up to 20 m s^{-1}) and low average irradiance (down to 100 µmol photons m^{-2} s^{-1}) between the two peaks in larval settlement and pre-ancestrulae abundance. Concomitantly, the temperature was stable in this period (around 8 °C), which may indicate that storms slowed down the settlement of larvae, making it harder for them to settle because of increased current speed and higher exposure. Moreover, M. I. Saunders and Metaxas (2010a) observed that spatial and temporal patterns in cyphonaute larvae distributions were influenced by density gradients in the water column. They observed that cyphonautes were more abundant in shallower, warmer and fresher layers when there was a strong pycnocline formed after a storm and suggested onshore transport during wind-driven downwelling events. Nalia Hama (2024) studied the cyphonaute abundance in the water in the same area location (MI) and period. Observations showed that also larval abundance in the water column was low during the stormy period (late May - beginning of June, figure 4.2.1).

The settlement was likely influenced by various factors, among which larvae transport and dispersal played a significant role. Attridge et al. (2022) observed a higher peak in settlement at higher wave exposures and suggested that it was because more wave action caused larger transport of passive larvae. Hydrodynamics, including vertical migration and dispersal strategies, have been shown to have an impact on shellfish larval dispersal. For example, Robins et al. (2013) showed that larvae that originated from exposed areas were able to migrate offshore and disperse further than larvae that remained in the flood-dominant estuaries. In the case of the cyphonaute larvae, which are obligatory

planktotrophic, hydrodynamics and dispersal are survival strategies as long as there is enough food (phytoplankton) in the water. This could mean that, for highly productive regions such as Frøya waters (Fragoso et al., 2019), the larvae likely largely rely on dispersal and finding a suitable substrate for settlement.

Abelson (1997) described that the cyphonaute larvae are able to explore the substrate in flow velocities that are faster than their locomotion speed. Also, the motion they prefer on the top of the kelp lamina is upstream. The larvae use their pyriform organ to navigate and to attach to the lamina while moving forward, by secreting mucus. Abelson (1997) suggests that the settlement itself is not only determined by currents but largely by a cue. The cyphonaute larva, when competent, responds to the environment (Hadfield et al., 2001) and it is known that settlement is also depending on chemical factors such as nutrient availability and chemoreception (Soule and Soule, 1977). Strathmann et al. (2008) observed that the structures of the cyphonaute (pyriform organ and internal sac) that were required for settlement and metamorphosis got smaller through a period of starvation but grew back when food was available again. Structures for swimming and feeding, on the other hand, were retained during starvation and the larva only metamorphosed if there was food available again. This indicates that the larva can survive for long periods without food and can extend the metamorphosis until the internal structures are big enough.

Almost all of the settled larvae and pre-ancestrulae was found on the meristem, the newer part of the lamina, for the whole sampling period and other studies observed the same (Denley et al., 2014; Matsson, 2020). Denley et al.(2014) suggested that the larva can probably detect the difference in the quality of kelp and have a preference for the newer part of the lamina because the coverage of colonies was uniform over the whole length of the kelp. Also, heavier fouling was observed on the older part of the lamina because colonies are older, meaning that they were growing when the seaweed was growing as well. This likely causes larvae to settle on the newer part of the lamina as there is more space and less competition, and they have the maximum time to grow before the lamina sheds the tips (Matsson, 2020).

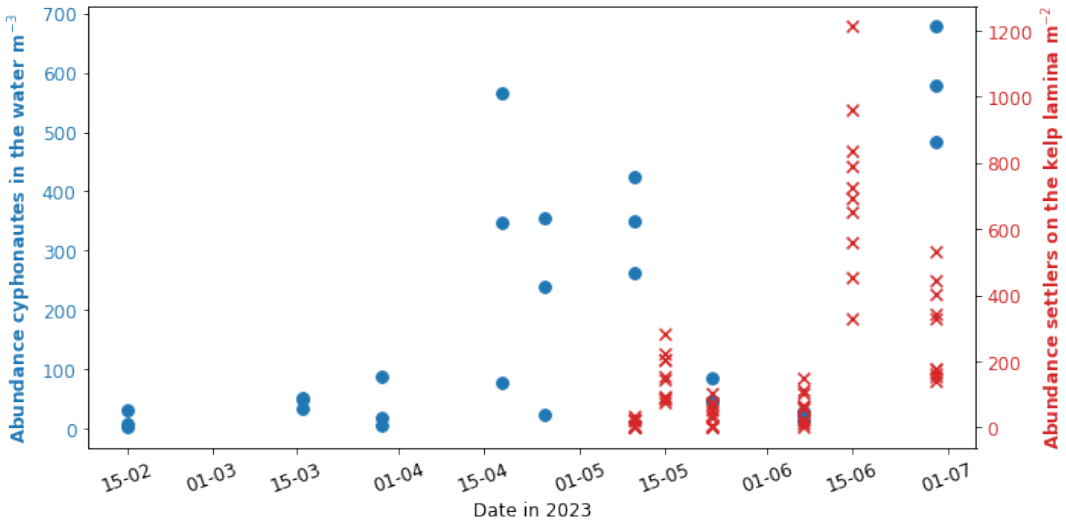

Figure 4.2.1: Graph showing the total cyphonaute abundance in the water (m^{-3}) in blue (data from Hama, 2024, counts are conducted by a taxonomist) and the larval settlement and pre-ancestrulae abundance per m^2 kelp lamina in red. Both deployment lines are included for the larval settlement and pre-ancestrulae abundance.

4.3 Bryozoan coverage

The percentage coverage remained below 1% until the beginning of June and sharply increased until the end of June 29^{th} (figure 3.3.1a). The data showed an increase in variation between the replicates when percentage coverage increases. For the line that was deployed in October, it had variations between 0.05% - 1.02% for the 7^{th} of June and 4.67% - 16.08% for the 29^{th} of June. For the January deployment line, the variation was 0.00% - 0.82% for the 7^{th} of June and 1.05% - 4.12% for the 29^{th} of June. The exponential trend of the data, as well as the variation in the data, corresponds with previous studies where percentage coverage was measured in the same area (Frøya and Skjøra) only with a different method (Førde, 2014; Njåstad, 2018).

Physical factors like hydrodynamics and topography are seen to have an effect on biofouling. Visch et al. (2020) observed a decrease in biofouling of epiphytes (10% and 6% coverage to 3%) in areas that were more exposed to waves and currents. In contrast with Matsson et al. (2019), who observed higher fouling of epiphytes in the more exposed areas (approximate difference of 16% and 61%). For both studies, the variation in coverage was high between the locations, even if the distance in location was small (20 km away for Visch et al., 2020 and 50 km away for Matsson et al. 2019). Attridge et al. (2022) observed the same level of coverage of *M. membranacea* on different wild kelp species for different ranges of wave exposure in Nova Scotia. In the Måsskjæra farm from Seaweed Solutions, a difference in biofouling was observed between different locations within the farm (approximately 100 meters away (Raposo, Seaweed Solutions, pers comm.). This all indicates that site selection for seaweed production while taking biofouling into consideration is complex.

The percentage coverage for the line deployed in October 2022 was overall higher compared with the line deployed in January 2023 (figure 3.3.1a). Also, the colony abundance

was higher for October (an increase of 22 counts a day and an increase of 15 counts a day for January) with more colonies bigger in size (figure 3.4.1). Bigger colonies grow faster; this growth is exponential and thus creates a higher coverage (M. Saunders and Metaxas, 2007; Hermansen et al., 2001; Riisgård and Goldson, 1997). The length of the October replicates was also larger (figure 3.2.1a). Matsson et al. (2019) observed a higher coverage at the more exposed site where kelp biomass was higher compared to other sites in Northern Norway. The reason for this could be that higher biomass (thus higher kelp density) affects wave exposure (Visch et al., 2020), creating less water flow around a higher density of kelp making it easier for larvae to settle. Matsson et al. (2021) observed that earlier deployment times (February compared with April and May) gave a higher biomass of *S. latissima*, but a lower carbon content, a lower relative daily shedding rate and higher coverage of biofouling. There was no effect of internal nitrate. The study suggested that the difference in the biofouling could be a relationship between the timing of the supply of larvae and the turnover time of the lamina caused by different growth and shedding rates. Another factor could be that the seaweed that was deployed in October is more nutrient-limited (less internal nitrate storage) because of the bigger size of the lamina and, thus, more susceptible to fouling. Although, there is no evidence in the literature that shows more vulnerability to fouling related to the overall health status of the kelp.

From all the environmental variables, temperature showed the highest positive correlation with the percentage coverage (figure 3.5.1). Likewise, cumulative temperature had the highest influence on the difference in percentage coverage between the dates (table 3.5.1). This is in line with findings in other studies (Matsson et al., 2019; M. Saunders and Metaxas, 2007). M. I. Saunders et al. (2010b) developed a model that predicted the effect of temperature differences on the coverage of *M. membranacea*. They predicted that an increase in 1-degree and 2-degree in the overall temperature resulted in an increase of coverage by a factor of 9 and 62, respectively, and earlier settlement in spring.

A negative effect of cumulative Chl *a* and weak negative correlation of Chl *a* with the bryozoan coverage was observed in this project (table 3.5.1; figure 3.5.1). This could make sense as no correlation was expected if Chl *a* levels are adequate enough for bryozoan to eat. The increase in temperature influenced the onset of spring bloom at the end of April. After the spring bloom in April, when bryozoan measurements started, the Chl *a* fluctuated around 2 mg m^{-3}. A linear relationship will be expected at low Chl *a* levels, but no low levels of Chl *a* were measured in this area. Frøya is a reproductive area because the NAW brings nutrient-rich water to the area and this water reaches the surface when there is coastal upwelling or internal waves. The area is known to contain high levels of primary production (Fragoso et al., 2019).

Bryozoan colonies are suspension feeders and need an ambient water flow to receive an optimal food intake for growth. Wilson-Ormond et al. (1997) observed that low water velocities limit the flux of food particles coming by for suspension-feeding oysters for them to catch, resulting in slower growth rates. The study suggested that the water velocity was more important for the flux than the amount of food available. On the other hand, Hermansen et al. (2001) observed no difference in colony growth when *E. pilosa* was exposed to increased water flow velocities (observations from 30 cm s^{-1} up to 150 cm s^{-1}). Also, lower algal concentrations (1.3 µg Chl *a* L^{-1}) still gave a maximum growth rate for *E. pilosa*. Saunders and Metaxas (2009) observed an interaction effect

between temperature and food, where a limitation of food only resulted in a smaller colony diameter at higher temperatures. This indicates that relationships between environmental variables (temperature, Chl *a*, current velocity) can affect the feed intake of bryozoans. But, this exact relationship is not clear and needs more research.

4.4 Future work and perspectives

This project showed that it is possible to detect early settlement of the larvae on the lamina by using a simple scanner. Here, bryozoan colonies, larval settlement and preancestrulae were quantified and digitized. This method has the potential to create a standardization among different farms in Norway and within different locations within a farm to gain more information about the biofouling of bryozoan colonies in seaweed farms. This is something crucial for modelling and predicting biofouling on seaweed in the future. Despite the method being time-consuming on its first try, with innovative machine learning techniques and effective sampling and digital image analysis, this method could be suitable for creating a bigger database of biofouling within farms.

In this study, no distinction is made between the two specimens, *E. pilosa* and *M. membranacea*. It was observed that for this cultivation period, the coverage of the two specimens was 50/50. Each year, farmers observe differences in the abundance of biofouling of the two different species on the kelp lamina (pers comm, Seaweed Solutions). This is interesting because it is known that *M. membranacea* has a preference for *S. latissima* to settle (Hayward and Ryland, 2017). Still, the images from this project can be used to get an exact distinction of these two species for this year.

Overall, the total sample dates (thus sample size, N = 7, cumulative, N = 5) were small. This made it difficult to find a statistical model that properly fitted the data to investigate the effect of the key environmental variables on the bryozoan coverage. The current statistical model (beta regression model and GLM) saw the higher values of percentage coverage as outliers, due to the small sample size. For this project a higher sample size was not possible as it was very much dependent on weather circumstances and time and availability during the harvest season. It is recommended that a sample size of at least 10 would be good in order to use bootstrapping or transformation of the data (Greenacre, 2016). Nevertheless, The number of dates was enough to observe the first settlement period and a clear exponential growth of the percentage coverage in time.

More research is needed to investigate whether the health state of the seaweed, salinity and nutrients affect bryozoan settlement and colony growth. Forbord et al. (2020) observed that biofouling occurred later at locations that were more influenced by freshwater inlets, and suggested that one of the life stages of *M. membranacea* could be affected by lower salinity levels.

Membranipora membranacea is an invasive species in Nova Scotia, Canada, and outbreaks of this specimen caused large losses of wild kelp beds. Climate change is expected to cause earlier and more abundant outbreaks of the species, which can have major implications for the ecosystem (M. Saunders and Metaxas, 2008). M. Saunders and Metaxas (2009) observed that settlement abundance increased after a warmer winter. Intensive farming increases the risk of kelp fronds breaking from the lines, falling down, and grow-

ing further in the area in the wild. This will lead to a higher abundance of bryozoan colonies in the area, and if climate change leads to warmer winters, this indicates that the survival rate for bryozoan colonies in this area will increase as well. This could lead to a higher and earlier sexual reproduction at the start of the season, which in terms can potentially lead to a higher settlement abundance and colony growth creating an earlier harvest and short growing season (less production) every year for the seaweed industry. Still, it is shown that the coverage can be variable and change every year probably because of currents and weather effects. For now, it is suggested to harvest when the water temperature gets above 8 °C (for this period) at the end of May in the coast of Trøndelag, assuming that the harvest takes up two weeks, to avoid a strong fouling that starts in June. This depends on the duration of the harvesting period, but also on the market, as higher percentage coverage on the kelp lamina can still be used for other market purposes besides food for humans, such as animal feed and bioenergy (Skjermo et al., 2014). The exact quantity of percentage coverage for different market purposes is not clear and needs more study. However, this can only be achieved if there is a standardized method for quantifying bryozoan coverage on the lamina.

Chapter 5

Conclusions

In this master's thesis project, a low-cost flatbed scanner was used successfully to digitize the larval settlement, pre-ancestrulae and colonies of the bryozoan species, *M. membranacea* and *E. pilosa*, on *S. latissima* lamina from a kelp farm in Frøya. The scanned images were used to detect settlement and pre-ancestrulae and gather accurate information about the total percentage of bryozoan coverage on the lamina and the abundance and size of the settled larvae, pre-ancestrulae and colonies. This was an exploratory method that, although time-consuming, allowed the detection of the smaller specimens ($<$ 1 mm). Further development that includes rapid image collection and automated detection creates the possibility to estimate bryozoan growth on a national scale, where knowledge would be built on how early and fast biofouling occurs within and across seaweed farms in Norway.

The results showed that the first settlement of the cyphonaute larva was observed at the end of April 2023. The first colonies were observed at the beginning of May 2023 and bryozoan colony abundance gradually increased over the whole sampling period. Percentage coverage stayed low ($<$ 1%) until the beginning of June and was followed up by an exponential increase until the end of June (11% and 3% average coverage). The observed colony size increased exponentially over time, but the overall highest size abundance was in the range of the smallest colonies ($<$ 0.5 in log + 1 mm^2).

The study indicated that storms (high wind speed, low irradiance and strong water mixing) likely negatively affected the settlement and development of the cyphonaute larvae on the lamina and that there was a strong correlation between bryozoan coverage and average temperature. The cumulative temperature was shown to have a significant influence on the percentage coverage and abundance with respect to every sampling date. Furthermore, the line that was deployed in January 2023 had a significant overall lower percentage coverage compared with October 2022. Although the average temperature had a positive correlation with bryozoan coverage, the coverage was not linearly related with chlorophyll *a*, suggesting that, as long as there is enough food (in the case of this study chlorophyll $a \geq 2$ mg m^{-3}, other factors (e.g. temperature, current speed) interplay.

It is expected that seawater temperature will increase because of climate change. This imposes a major challenge in seaweed aquaculture, as the life cycle of many biofouling organisms, including bryozoan, is strongly connected to temperature changes. Higher temperatures could lead to an earlier start of sexual reproduction of bryozoans in the spring, an earlier settlement and an increase in the growth rates of bryozoan colonies

on the lamina. Moreover, warmer winters can potentially increase the survival rates of bryozoan colonies in the area, causing a higher abundance of larval stock (overall bryozoan populations). This could shorten the kelp growing season. For prediction purposes, more research is needed to investigate relationships between the environmental variables and the effect of the hydrodynamics of the area on bryozoan settlement and coverage.

Bibliography

Abelson, A. (1997). Settlement in Flow: Upstream Exploration of Substrata by Weakly Swimming Larvae. *Ecology*, *78*(1), 160–166.

Albrecht, M. (2023). A Norwegian seaweed utopia? Governmental narratives of coastal communities, upscaling, and the industrial conquering of ocean spaces. *Maritime Studies*, *22*(3). https://doi.org/10.1007/s40152-023-00324-2

Atkins, D. (1955). The Cyphonautes larvae of the plymouth area and the metamorphosis of Membranipora Membranacea (L.) *Journal of the Marine Biological Association of the United Kingdom*, *34*(3), 441–449.

Attridge, C. M., Metaxas, A., & Denley, D. (2022). Wave exposure affects the persistence of kelp beds amidst outbreaks of the invasive bryozoan Membranipora membranacea. *Marine Ecology Progress Series*, *702*, 39–56. https://doi.org/10.3354/meps14191

Bak, U. G., Mols-Mortensen, A., & Gregersen, O. (2018). Production method and cost of commercial-scale offshore cultivation of kelp in the Faroe Islands using multiple partial harvesting. *Algal Research*, *33*, 36–47. https://doi.org/10.1016/j.algal.2018.05.001

Bannister, J., Sievers, M., Bush, F., & Bloecher, N. (2019). Biofouling in marine aquaculture: a review of recent research and developments. *Biofouling*, *35*(6), 631–648. https://doi.org/10.1080/08927014.2019.1640214

Bradski, G. (2000). The OpenCV Library. *Dr. Dobb's Journal of Software Tools*, *25*(11).

Burridge, M. (2012). *Biological Synopsis of the Lacy Crust Bryozoan (Membranipora membranacea)* [Doctoral dissertation].

Cohen, D. S. (2019, April). *The influence of bryozoan encrustation on the halogen content of cultivated Saccharina latissima* (tech. rep.). Norwegian University of Science and Technoloy. Trondheim.

Denley, D., Metaxas, A., & Short, J. (2014). Selective settlement by larvae of Membranipora membranacea and Electra pilosa (Ectoprocta) along kelp blades in Nova Scotia, Canada. *Aquatic Biology*, *21*(1), 47–56. https://doi.org/10.3354/ab00569

Directorate of Fisheries. (2023). Algae. https://www.fiskeridir.no/English/Aquaculture/Statistics/Algae

FAO. (2021, December). The need for guidance on alternative proteins highlighted to Codex Alimentarius Commission. https://www.fao.org/in-action/sustainable-and-circular-bioeconomy/resources/news/details/en/c/1459357/

FAO. (2022). *The State of World Fisheries and Aquaculture 2022. Towards Blue Transformation.* (tech. rep.). FAO. Rome. https://doi.org/https://doi.org/10.4060/cc0461en

Forbord, S., Matsson, S., Brodahl, G. E., Bluhm, B. A., Broch, O. J., Handå, A., Metaxas, A., Skjermo, J., Steinhovden, K. B., & Olsen, Y. (2020). Latitudinal, seasonal and depth-dependent variation in growth, chemical composition and biofouling of cultivated Saccharina latissima (Phaeophyceae) along the Norwegian coast. *Journal of Applied Phycology*, *32*(4), 2215–2232. https://doi.org/10.1007/s10811-020-02038-y

Forbord, S., Steinhovden, K., Kjølbo Rød, K., Handå, A., & Skjermo, J. (2018, April). Cultivation protocol for Saccharina latissima. In *Protocols for macroalgae research* (1st ed., pp. 37–59). CRC Press.

Førde, H. (2014, May). *Development of bryozoan fouling on cultivated kelp (Saccharina latissima) in Norway* (tech. rep.). Norwegian University of Science and Technology. Trondheim.

Førde, H., Forbord, S., Handå, A., Fossberg, J., Arff, J., Johnsen, G., & Reitan, K. I. (2016). Development of bryozoan fouling on cultivated kelp (Saccharina latissima) in Norway. *Journal of Applied Phycology*, *28*(2), 1225–1234. https://doi.org/10.1007/s10811-015-0606-5

Fragoso, G. M., Davies, E. J., Ellingsen, I., Chauton, M. S., Fossum, T., Ludvigsen, M., Steinhovden, K. B., Rajan, K., & Johnsen, G. (2019). Physical controls on phytoplankton size structure, photophysiology and suspended particles in a Norwegian biological hotspot. *Progress in Oceanography*, *175*, 284–299. https://doi.org/10.1016/j.pocean.2019.05.001

Franzén, Å. (1977). Gametogenesis of Bryozoans. In R. Woollacott & R. Zimmer (Eds.), *Biology of bryozoans* (pp. 1–21). Academic Press, Inc.

Greenacre, M. (2016). Data reporting and visualization in ecology. *Polar Biology*, *39*(11), 2189–2205. https://doi.org/10.1007/s00300-016-2047-2

Hadfield, M. G., Carpizo-Ituarte, E. J., Del Carmen, K., & Nedved, B. T. (2001). Metamorphic Competence, a Major Adaptive Convergence in Marine Invertebrate Larvae. *American Zoologist*, *41*(5), 1123–1131. https://academic.oup.com/icb/article/41/5/1123/342969

Hama, N. (2024, May). *Using a low-cost high throughput microscope in cultivated seaweed farms for early biofouling detection.* (tech. rep.). Norwegian University of Science and Technology. Trondheim.

Harris, C. R., Millman, K. J., van der Walt, S. J., Gommers, R., Virtanen, P., Cournapeau, D., Wieser, E., Taylor, J., Berg, S., Smith, N. J., Kern, R., Picus, M., Hoyer, S., van Kerkwijk, M. H., Brett, M., Haldane, A., del Río, J. F., Wiebe, M., Peterson, P., ... Oliphant, T. E. (2020). Array programming with NumPy. *Nature*, *585*(7825), 357–362. https://doi.org/10.1038/s41586-020-2649-2

Harvell, C. D., & Helling, R. (1993). Experimental Induction of Localized Reproduction in a Marine Bryozoan. *Biol Bull.*, *184*(3), 286–295.

Hassan, R. (2024, May). *Automated Segmentation of Bryozoan Colonies and Prediction of Growth in Kelp Farms* (tech. rep.). Oslo Metropolitan University. Oslo.

Hayward, P. J., & Ryland, J. S. (2017, February). Bryozoa. In *Handbook of the marine fauna of north-west europe* (2nd ed., pp. 603–638). Oxford University Press. https://doi.org/10.1093/acprof:oso/9780199549443.003.0011

Hermansen, P., Larsen, P. S., & Riisgård, H. U. (2001). Colony growth rate of encrusting marine bryozoans (Electra pilosa and Celleporella hyalina). *Journal of Experimental Marine Biology and Ecology*, *263*, 1–23. https://doi.org/10.1016/S0022-0981(01)00243-X

Hickman, C., Keen, S., Eisenhour, D., Larson, A., & I'Anson, H. (2017). Polyzoa and Kryptrochozoa. In *Integrated principles of zoology* (17th ed., pp. 319–324). McGraw-Hill Education.

Hunter, J. D. (2007). Matplotlib: A 2D Graphics Environment. *Computing in Science & Engineering*, *9*(3), 90–95. https://doi.org/10.1109/MCSE.2007.55

Inkscape Project. (2020). Inkscape. https://inkscape.org/

Kérouel, R., & Aminot, A. (1997). Fluorometric determination of ammonia in sea and estuarine waters by direct segmented flow analysis. *Marine Chemistry*, *57*, 265–275.

Kirillov, A., Mintun, E., Ravi, N., Mao, H., Rolland, C., Gustafson, L., Xiao, T., Whitehead, S., Berg, A. C., Lo, W.-Y., Dollár, P., & Girshick, R. (2023, April). *Segment Anything* (tech. rep.). Meta AI Research, FAIR. https://segment-anything.com.

Koesling, M., Kvadsheim, N. P., Halfdanarson, J., Emblemsvåg, J., & Rebours, C. (2021). Environmental impacts of protein-production from farmed seaweed: Comparison of possible scenarios in Norway. *Journal of Cleaner Production*, *307*. https://doi.org/10.1016/j.jclepro.2021.127301

Lomartire, S., Marques, J. C., & Gonçalves, A. M. (2021). An overview to the health benefits of seaweeds consumption. *Marine Drugs*, *19*(6). https://doi.org/10.3390/md19060341

Matsson, S., Christie, H., & Fieler, R. (2019). Variation in biomass and biofouling of kelp, Saccharina latissima, cultivated in the Arctic, Norway. *Aquaculture*, *506*, 445–452. https://doi.org/10.1016/j.aquaculture.2019.03.068

Matsson, S., Metaxas, A., Forbord, S., Kristiansen, S., Handå, A., & Bluhm, B. A. (2021). Effects of outplanting time on growth, shedding and quality of Saccharina latissima (Phaeophyceae) in its northern distribution range. *Journal of Applied Phycology*, *33*, 2415–2431. https://doi.org/10.1007/s10811-021-02441-z/Published

Matsson, S. (2020). *Fouling of macro epibionts on cultivated Saccharina latissima (Phaeophyceae) In situ temporal and spatial variation* [Doctoral dissertation, The Arctic University of Norway].

McKinney, W., & & Others. (2010). Data structures for statistical computing in python. *Proceedings of the 9th Python in Science Conference*, 51–56.

Njåstad, E. B. (2018, May). *Influence of food availability and nutritional state of macroalgae on development of fouling bryozoans on cultivated Saccharina latissima* (tech. rep.). Norwegian University of Science and Technology. Trondheim.

Norwegian Centre for Climate Services. (n.d.). Seklima Observations and weather statistics. https://seklima.met.no/

Plotly Technologies Inc. (2015). Collaborative data science. https://plot.ly

R Core Team. (2024). R: A Language and Environment for Statistical Computing. https://www.R-project.org/

Riisgård, H. U., & Goldson, A. (1997). Minimal scaling of the lophophore filter-pump in ectoprocts (Bryozoa) excludes physiological regulation of filtration rate to nutritional needs. Test of hypothesis. *Marine Ecology Progress Series*, *156*, 109–120.

Rioux, L. E., Beaulieu, L., & Turgeon, S. L. (2017, July). Seaweeds: A traditional ingredients for new gastronomic sensation. https://doi.org/10.1016/j.foodhyd.2017.02.005

Robins, P. E., Neill, S. P., Giménez, L., Stuart, R., Jenkins, S. R., & Malham, S. K. (2013). Physical and biological controls on larval dispersal and connectivity in a

highly energetic shelf sea. *Limnology and Oceanography*, *58*(2), 505–524. https://doi.org/10.4319/lo.2013.58.2.0505

RStudio Team. (2020). RStudio: Integrated Development Environment for R. http://www.rstudio.com/

Ryland, J. S., & Stebbing, A. R. D. (1971). Settlement and orientated growth in epiphytic and epizoic bryozoans. *Fourth European Marine Biology Symposium*, 105–123. https://www.researchgate.net/publication/284108942

Ryland, J. (1965). *Polyzoa (Bryozoa) order cheilostomata cyphonautes larvae Zooplankton sheet 107* (tech. rep.). https://doi.org/10.17895/ices.pub.4948

Saether, M., Diehl, N., Monteiro, ·. C., Li, H., Niedzwiedz, S., Bertille Burgunter-Delamare, ·., Scheschonk, L., Bischof, K., & Forbord, S. (2024). The sugar kelp Saccharina latissima II: Recent advances in farming and applications. *Journal of Applied Phycology*. https://doi.org/10.1007/s10811-024-03213-1

Sætre, R. (2007). Driving forces. In *The norwegian coastal current - oceanography and climate* (pp. 45–58). Tapir Academic Press Institute of Marine Research.

Saifullah, Olsen, Y., Surilayani, D., & Handå, A. (2021). Carbohydrate of the Brown Seaweed, Saccharina latissima: A Review. https://www.sintef.no/projectweb/macrosea/

Santagata, S. (2015). Ectoprocta. In *Evolutionary developmental biology of invertebrates 2* (pp. 247–262). Springer Vienna. https://doi.org/10.1007/978-3-7091-1871-9{_}11

Saukshaug, E., Johnsen, G., & Kovacs, K. (2009). Appendix A. Units. In *Ecosystem barents sea*. Tapir Academic Press.

Saunders, M., & Metaxas, A. (2007). Temperature explains settlement patterns of the introduced bryozoan Membranipora membranacea in Nova Scotia, Canada. *Marine Ecology Progress Series*, *344*, 95–106. https://doi.org/10.3354/meps06924

Saunders, M., & Metaxas, A. (2008). High recruitment of the introduced bryozoan Membranipora membranacea is associated with kelp bed defoliation in Nova Scotia, Canada. *Marine Ecology Progress Series*, *369*, 139–151. https://doi.org/10.3354/meps07669

Saunders, M. I., & Metaxas, A. (2010). Physical forcing of distributions of bryozoan cyphonautes larvae in a coastal embayment. *Marine Ecology Progress Series*, *418*, 131–145. https://doi.org/10.3354/meps08842

Saunders, M. I., Metaxas, A., & Filgueiraa, R. (2010). Implications of warming temperatures for population outbreaks of a nonindigenous species (Membranipora membranacea, Bryozoa) in rocky subtidal ecosystems. *Limnology and Oceanography*, *55*(4), 1627–1642. https://doi.org/10.4319/lo.2010.55.4.1627

Saunders, M., & Metaxas, A. (2009). Effects of temperature, size, and food on the growth of Membranipora membranacea in laboratory and field studies. *Marine Biology*, *156*(11), 2267–2276. https://doi.org/10.1007/s00227-009-1254-6

Shevchenko, E. T., Varfolomeeva, M. A., Nekliudova, U. A., Kotenko, O. N., Usov, N. V., Granovitch, A. I., & Ostrovsky, A. N. (2020). Electra vs Callopora: life histories of two bryozoans with contrasting reproductive strategies in the White Sea. *Invertebrate Reproduction and Development*, *64*(2), 137–157. https://doi.org/10.1080/07924259.2020.1729260

Sjøtun, K. (1993). Seasonal Lamina Growth in two Age Groups of Laminaria saccharina (L.) Lamour. in Western Norway. *Botanica Marina*, *36*, 433–441. https://doi.org/10.1515/botm.1993.36.5.433

Skjermo, J., Aasen, I. M., Arff, J., Broch, O. J., Carvajal, A., Christie, H., Forbord, S., Olsen, Y., Reitan, I., Rustad, T., Sandquist, J., Solbakken, R., Steinhovden, K. B., Wittgens, B., Wolff, R., & Handå, A. (2014, September). *A new Norwegian bioeconomy based on cultivation and processing of seaweeds: Opportunities and R&D needs* (tech. rep.). SINTEF. Trondheim, Norway.

Smithson, M., & Verkuilen, J. (2006). Supplemental Material for A Better Lemon Squeezer? Maximum-Likelihood Regression With Beta-Distributed Dependent Variables. *Psychological Methods*. https://doi.org/10.1037/1082-989x.11.1.54.supp

Soule, J., & Soule, D. (1977). Fouling and Bioadhesion: Life Strategies of Bryozoans. In R. Zimmer & R. Woollacott (Eds.), *Biology of bryozoans* (pp. 437–453). Academic Press, Inc.

Stévant, P., Rebours, C., & Chapman, A. (2017). Seaweed aquaculture in Norway: recent industrial developments and future perspectives. *Aquaculture International*, *25*(4), 1373–1390. https://doi.org/10.1007/s10499-017-0120-7

Strathmann, R. R., Foley, G. P., & Hysert, A. N. (2008). Loss and gain of the juvenile rudiment and metamorphic competence during starvation and feeding of bryozoan larvae. *Evolution and Development*, *10*(6), 731–736. https://doi.org/10.1111/j.1525-142X.2008.00287.x

Stricker, S. A. (1989). Settlement and metamorphosis of the marine bryozoan Membranipora Membranacea. *Bulletin of Marine Science*, *45*(2), 387–405.

Ström, R. (1977). Brooding Patterns of Bryozoans. In R. Zimmer & R. Woollacott (Eds.), *Biology of bryozoans* (pp. 23–52). Academic Press, Inc.

Thomas, J. B., Sodré Ribeiro, M., Potting, J., Cervin, G., Nylund, G. M., Olsson, J., Albers, E., Undeland, I., Pavia, H., & Gröndahl, F. (2021). A comparative environmental life cycle assessment of hatchery, cultivation, and preservation of the kelp Saccharina latissima. *ICES Journal of Marine Science*, *78*(1), 451–467. https://doi.org/10.1093/icesjms/fsaa112

Thomason, B. P. (2023, May). *Bryozoan larvae (cyphonauts) growth and encrustation in Saccharina latissima: analysis of biotic and abiotic interactions* (tech. rep.). Norwegian University of Science and Technology. Trondheim.

Van Rossum, G., & Drake Jr, F. (1955). *Python reference manual*. Centrum voor Wiskunde en Informatica Amsterdam.

Vassbotn Kamfjord, B. (2002, April). *Fotograferingsteknikk og programutvikling av bildebehandingsverktoy til numeriske studier av vekst og slitasje hos mosdyrene Membranipora membranacea og Electra pilosa (Bryozoa)* (tech. rep.). Norwegian University of Science and Technology. Trondheim.

Vaughan, K. (2020, February). Compare CCD vs CIS Scanning Technologies. https://www.tavco.net/articles/bid/107329/compare-ccd-vs-cis-scanner-technologies

Verdegem, M., Buschmann, A. H., Latt, U. W., Dalsgaard, A. J., & Lovatelli, A. (2023). The contribution of aquaculture systems to global aquaculture production. *Journal of the World Aquaculture Society*, *54*(2), 206–250. https://doi.org/10.1111/jwas.12963

Visch, W., Nylund, G. M., & Pavia, H. (2020). Growth and biofouling in kelp aquaculture (Saccharina latissima): the effect of location and wave exposure. *Journal of Applied Phycology*, *32*(5), 3199–3209. https://doi.org/10.1007/s10811-020-02201-5

Volent, Z., Johnsen, G., Hovland, E. K., Folkestad, A., Olsen, L. M., Tangen, K., & Sorensen, K. (2011). Improved monitoring of phytoplankton bloom dynamics in a Norwegian fjord by integrating satellite data, pigment analysis, and Ferrybox data

with a coastal observation network. *Journal of Applied Remote Sensing*, *5*(1), 1. https://doi.org/10.1117/1.3658032

Waskom, M. (2021). seaborn: statistical data visualization. *Journal of Open Source Software*, *6*(60), 3021. https://doi.org/10.21105/joss.03021

Wassick, A., Hunsucker, K. Z., & Swain, G. (2023). Measuring the recruitment and growth of biofouling communities using clear recruitment panels. *Biofouling*, *39*(6), 643–660. https://doi.org/10.1080/08927014.2023.2243236

Wilson-Ormond, E. A., Powell, E. N., & Ray, S. M. (1997). Short-term and small-scale variation in food availability to natural oyster populations: Food, flow and flux. *Marine Ecology*, *18*(1), 1–34. https://doi.org/10.1111/j.1439-0485.1997.tb00424.x

Winston, J. (1977). Feeding in Marine Bryozoans. In R. Zimmer & R. Woollacott (Eds.), *Biology of bryozoans* (pp. 233–268). Academic Press, Inc.

Yorke, A. F., & Metaxas, A. (2011). Interactions between an invasive and a native bryozoan (Membranipora membranacea and Electra pilosa) species on kelp and Fucus substrates in Nova Scotia, Canada. *Marine Biology*, *158*(10), 2299–2311. https://doi.org/10.1007/s00227-011-1734-3

Yoshioka, P. M. (1982). Role of Planktonic and Benthic Factors in the Population Dynamics of the Bryozoan Membranipora Membranacea. *Ecology*, *63*(2), 457–468. https://doi.org/https://doi.org/10.2307/1938963

Zimmer, R., & Woollacott, R. (1977). Metamorphosis, Ancestrulae, and Coloniality in Bryozoan Life Cycles. In R. Zimmer & R. Woollacott (Eds.), *Biology of bryozoans* (pp. 91–139). Academic Press, Inc.

Appendices

A - Github repository

The Github repository link below includes all the code used to retrieve data about bryozoan colonies, recruitment, and the percentage of bryozoan coverage from the SVG files. This repository also includes the method for the kelp area estimation from the images and recruitment and colony sizes.

Github repository link

- https://github.com/Elisabeth-AliceS/BryozoanCoverage

B - Data tables used for statistics

B1 - data used for statistical models

Table B.1: The data used for the statistical models

Day	Line	Delta % Coverage	Delta Counts	Cum. Temp.	Cum. *chl a*	Cum. Turbidity
15	Oct	0.007	168	95.77	24.45	1.40
20	Oct	0.017	61	37.14	10.80	0.81
28	Oct	0.041	258	66.13	15.53	1.05
43	Oct	0.461	104	121.58	28.02	2.12
51	Oct	1.511	372	71.10	14.33	1.47
65	Oct	9.193	296	147.90	23.96	2.75
20	Jan	0.012	83	37.14	10.80	0.81
28	Jan	0.011	20	66.13	15.53	1.05
43	Jan	0.199	84	121.58	28.02	2.12
51	Jan	1.044	401	71.10	14.33	1.47
65	Jan	1.654	194	147.90	23.96	2.75

B2 - data used for correlation matrices

sample	date	day	line	% coverage	colony counts	recruitment counts
1	10/05/2023	15	oct	0.006	117	33
2	10/05/2023	15	oct	0.008	109	6
3	10/05/2023	15	oct	0.004	121	0
4	10/05/2023	15	oct	0.01	304	20
5	10/05/2023	15	oct	0.007	189	25
1	15/05/2023	20	oct	0.023	259	155
2	15/05/2023	20	oct	0.022	216	206
3	15/05/2023	20	oct	0.036	255	222
4	15/05/2023	20	oct	0.026	200	145
5	15/05/2023	20	oct	0.018	217	207
1	23/05/2023	28	oct	0.074	479	77
2	23/05/2023	28	oct	0.067	371	0
3	23/05/2023	28	oct	0.069	551	102
4	23/05/2023	28	oct	0.044	386	66
5	23/05/2023	28	oct	0.073	651	52
1	07/06/2023	43	oct	0.055	223	22
2	07/06/2023	43	oct	0.231	455	148
3	07/06/2023	43	oct	0.893	934	65
4	07/06/2023	43	oct	0.433	455	103
5	07/06/2023	43	oct	1.017	892	64
1	15/06/2023	51	oct	2.086	1084	837
2	15/06/2023	51	oct	2.574	1283	961
3	15/06/2023	51	oct	1.634	1014	790
4	15/06/2023	51	oct	2.296	865	1214
5	15/06/2023	51	oct	1.595	575	330
1	29/06/2023	65	oct	16.077	1421	530
2	29/06/2023	65	oct	13.386	1965	446
3	29/06/2023	65	oct	4.669	775	178
4	29/06/2023	65	oct	10.075	1095	401
5	29/06/2023	65	oct	11.945	1047	343
1	10/05/2023	15	jan	0.002	95	0
2	10/05/2023	15	jan	0.001	26	0
3	10/05/2023	15	jan	0.001	32	0
4	10/05/2023	15	jan	0.005	190	24
5	10/05/2023	15	jan	0.001	48	0
1	15/05/2023	20	jan	0.014	188	90
2	15/05/2023	20	jan	0.007	110	76
3	15/05/2023	20	jan	0.021	225	285
4	15/05/2023	20	jan	0.012	160	96
5	15/05/2023	20	jan	0.015	125	84
1	23/05/2023	28	jan	0.031	152	38
2	23/05/2023	28	jan	0.033	214	0
3	23/05/2023	28	jan	0.007	96	0
4	23/05/2023	28	jan	0.037	240	8

5	23/05/2023	28	jan	0.016	209	30
1	07/06/2023	43	jan	0.048	118	26
2	07/06/2023	43	jan	0.819	611	56
3	07/06/2023	43	jan	0.11	301	113
4	07/06/2023	43	jan	0.005	52	0
5	07/06/2023	43	jan	0.134	250	10
1	15/06/2023	51	jan	2.377	939	652
2	15/06/2023	51	jan	0.948	461	560
3	15/06/2023	51	jan	0.983	625	455
4	15/06/2023	51	jan	1.323	813	725
5	15/06/2023	51	jan	0.704	499	695
1	29/06/2023	65	jan	4.077	1327	331
2	29/06/2023	65	jan	2.05	747	140
3	29/06/2023	65	jan	3.315	907	154
4	29/06/2023	65	jan	4.117	991	177
5	29/06/2023	65	jan	1.046	338	164

Table B.2: The data used for the correlation matrices

B3 - average values of the sensor data used for correlation matrices

date	temperature	chl a	turbidity
10/05/2023	7.28	2.35	0.12
15/05/2023	7.82	2.45	0.15
23/05/2023	8.51	2.08	0.14
07/06/2023	8.42	1.94	0.13
15/06/2023	10.16	2.37	0.24
29/06/2023	11.7	1.27	0.09

Table B.3: Values of the average temperature, Chl *a* and turbidity for the different dates retrieved from the sensor data. This data is used for correlation matrices.

NTNU

Norwegian University of
Science and Technology